DOI: 10.1002/ejoc.201100493

Foldamers Based on Oxazolidin-2-ones

Claudia Tomasini,*[a] Gaetano Angelici,[b] and Nicola Castellucci[a]

Keywords: Foldamers / Heterocycles / Helical structures / Peptidomimetics / Conformation analysis / Supramolecular chemistry

Foldamers are artificial molecules capable of organization into well defined secondary structures such as helixes, β sheets and turns. The essential requirement for an oligomer to qualify for inclusion in the foldamer family is to possess a well defined, repetitive secondary structure, imparted by conformational restrictions imposed by the monomeric unit. These compounds may be composed of subunits of any kind, but most of them contain unusual amino acids and/or aromatic units. We describe the synthesis, the conformation analysis and the physical properties (in the solid state) of pseudopeptide foldamers containing imido-type functions, obtained by coupling the nitrogen of a 4-carboxy oxazolidin-2-one unit with the carboxylic acid moiety of the next unit, which may be another 4-carboxy oxazolidin-2-one or an amino acid. Such an imido-type function is characterized by a nitrogen atom connected both to an endocyclic and to an exocyclic carbonyl group, and tends always to adopt the *trans* conformation. As a consequence of this remarkable property, which causes local constraint, these imido-type oligomers are forced to fold in ordered conformations. In combination with interactions of other kinds (H bond, apolar interactions, etc.), these lead to the formation of supramolecular materials. The synthetic approach is highly tuneable with endless variations, so materials with required properties may be prepared "on demand", simply by changing the design and the synthesis.

Introduction

The word "foldamers" was coined to describe discrete artificial oligomers that adopt specific and stable conformations akin to those seen among biopolymers such as proteins and nucleic acids.[1] This neologism means "folding molecules" and refers mainly to medium-sized molecules (about 500–5000 amu) that fold into definite secondary structures (i.e., helices, turns and sheets), thus being able to mimic biomacromolecules despite their smaller sizes. The essential requirement of a foldamer is to possess a well defined, repetitive secondary structure, imparted as a result of conformational restrictions of the monomeric unit.

Investigation into these new structural scaffolds has blossomed in many laboratories because they hold promise for addressing chemical, physico-chemical and biological problems and represent a new frontier in research.[2] Many groups have explored oligomers with wide backbone variety as potential foldamers. A large family of foldamers explored to date is that made up of oligomers derived from amino acid building blocks (including α-, β-, γ- and δ-amino acids);[3] this family (i.e., oligoamides) offers myriad possibilities for the construction of sophisticated folded architectures with possible applications ranging from biomedicine to materials science.[4] Recently, several examples of foldamers containing mixtures of α- and β-, α- and γ-, or β- and γ-amino acids in alternating order have been reported. As well as helical structures with hydrogen bonds pointing only in one direction, either backward or forward along the sequence, mixed helixes (β helixes) with hydrogen bonds alternately changing in forward and backward directions have also been found in these regular hybrid peptides.[5]

In the last few years the design and synthesis of oligomers based on proline units, both in the presence and absence of stabilizing hydrogen bonds, have been extensively pursued. As examples, non-hydrogen-bonded secondary structures such as poly(Pro)$_n$ helices occur occasionally in proteins and in short peptides, individual strands within the collagen triple helix are folded in a poly(Pro)$_n$ II (PPII) conformation, and short PPII helices play important roles in protein–protein recognition.

Interesting new structures may be prepared by replacing the proline moieties with pseudoproline (ΨPro) units.[6] This term was introduced recently to indicate synthetic proline analogues usually obtained by cyclocondensation of the amino acids cysteine, threonine or serine with aldehydes or ketones. The conformation preceding ΨPro in a peptide is a matter of interest because the propensity of the amino acid proline to form a Xaa$_{i-1}$–Pro$_i$ *cis* peptide bond can be strongly enhanced by the introduction of a pseudoproline residue. Very recently oxazolidines containing trifluoromethyl groups (Fox) have been synthesized by condensation of serine esters with trifluoroacetaldehyde hemiacetal or trifluoroacetone.[7]

[a] Dipartimento di Chimica "G. Ciamician"
Alma Mater Studiorum Università di Bologna
via Selmi 2, 40126 Bologna, Italy
Fax: +39-051-2099456
E-mail: claudia.tomasini@unibo.it
[b] Department of Chemistry, University of Basel,
St. Johanns-Ring 19, 4056 Basel, Switzerland

Five-membered cycles that contain a nitrogen and a carboxy unit adjacent to one another in the ring may be assigned to the family of pseudoprolines: all these compounds share the same properties because a nitrogen atom adjacent to a carbonyl group behaves as a rigid spacer, owing to the presence of the endocyclic carbonyl group, which strictly imposes a *trans* conformation on the adjacent peptide bond. This effect is due to the tendency of the two carbonyl groups to orient themselves apart from one another (Figure 1).

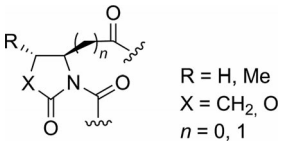

Figure 1. Preferential conformation of the imidic bond.

This microreview summarizes recent work on foldamers containing some pseudoproline units, such as pyroglutamic acid, 4-carboxyoxazolidin-2-ones or 4-carboxyimidazolidin-2-ones. The introduction of these heterocycles in oligomers causes local constraints that force the oligomers to fold in ordered conformations.

In the first and second parts of the review, the synthetic methods required to prepare and to derivatize these heterocycles are described. In the third part, the conformation analysis of these foldamers in solution is reported, whereas in the fourth part the behaviour of these foldamers as supramolecular materials is described.

The extensive study that has been performed on this group of foldamers allows the preparation of supramolecular materials with remarkable properties with different potential applications.

The synthetic approach is highly tuneable with endless variations, so foldamers with the required properties may be prepared "on demand" simply by changing the design and the synthesis.

1. Preparation of Oxazolidin-2-ones and Related Molecules

Several compounds possessing these properties have been prepared on middle to large scales. To allow the use of inexpensive natural compounds that are capable of forming imidic bonds, the possibility of utilizing pyroglutamic acid (*p*Glu) as a pseudoproline moiety was investigated.[8] Although *p*Glu is available in both configurations at low price, it is usually present in polypeptide chains only as an N-terminal amino acid, owing to the low reactivity of the nitrogen, and very few examples of nitrogen acylation have been described.[9] Unfortunately, the derivatization of pyroglutamic acid proved to be quite difficult (see Section 1.4) because it is an amide, so 2-carboxyoxazolidin-2-ones and 2-carboxyimidazolidin-2-ones were synthesized. These compounds are more reactive towards acylation, due to the reduction of nitrogen back-donation by the presence of another heteroatom adjacent to the carbonyl group.

1.1. Preparation of 5-Substituted *trans*-(4*S*,5*R*)-4-Carboxybenzyloxazolidin-2-ones (Oxd)

These compounds are common heterocycles[10] easily obtainable by treatment of vicinal amino alcohols with a synthetic equivalent of carbon dioxide,[11] provided that the amino alcohols are commercially available or can be easily synthesized.[12]

Claudia Tomasini was born and educated in Bologna (Italy). She received her chemistry degree cum laude in 1982 and her PhD in Organic Chemistry in 1986 at the Alma Mater Studiorum Università di Bologna (Italy). In 1987–1988 she worked as a postdoctoral associate with Professor Jack E. Baldwin at Dyson Perrins Laboratory, the University of Oxford, Oxford, UK. In 1990 she joined the Chemistry Department at the Università di Bologna as assistant professor, becoming associate professor in 1998. Her research interests include the synthesis of unusual amino acids, the preparation and conformational studies of pseudopeptide foldamers and analysis of the behaviour of synthetic oligomers in solution and in the solid state for the formation of supramolecular materials.

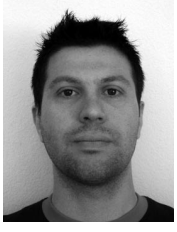

Gaetano Angelici was born in Porto San Giorgio, Italy. He obtained his degree in Chemistry (MSc) in 2005 from the University of Bologna, working with Prof. C. Trombini on "Cobalt-Catalysed Addition of Allylidene Dipivalate to Aldehydes". He then joined Prof. C. Tomasini's research group and completed his PhD thesis in 2008, on the "Synthesis and Conformational Analysis of Pseudopeptides able To Fold in Defined Secondary Structures". In 2009 he joined the group of Prof. H. Wennemers at the University of Basel (Switzerland), working on the "Development of New Organocatalysts Based on Peptides".

Nicola Castellucci was born in Urbino (Italy) in 1984. In December 2008 he received his master's degree in Advanced Chemical Methodologies from the University of Bologna under the direction of Prof. C. Trombini on "New Methods in Organocatalysis". In January 2009 he obtained a fellowship in Bologna working in the field of the synthesis of new pseudopeptides under the supervision of Prof. C. Tomasini. In 2010 he started on his PhD in the same group.

As well as a straightforward method that allows 5-methyl-4-carboxyoxazolidin-2-one to be obtained by starting from L-threonine,[13] a general synthetic method that affords any 5-substituted *trans*-(4*S*,5*R*)-4-carboxybenzyloxazolidin-2-one from an enantiomerically pure β-amino acid has been reported.[14]

N-Boc β-amino methyl acids can be easily obtained in enantiomerically pure form by enzymatic hydrolysis of the corresponding racemic *N*-phenylacetyl amide with penicillin G acylase (PGA),[15] which preferentially hydrolyses the L (i.e., *S*) enantiomer.

On treatment with LiHMDS and iodine at low temperature, the fully protected β-amino acids undergo cyclization with the formation of the corresponding 3-alkyl/aryl-substituted 2-carboxymethylaziridines with high diastereoselectivity (Scheme 1).[16] The reactions between the lithium dianions of *N*-protected β-amino esters and electrophiles afford the 2,3-*anti* adducts both in high yields and with high stereoselectivities, as previously reported.[17] When the electrophile is a good leaving group (as in the case of halogens), the direct formation of the corresponding aziridine is observed, because the halogen is substituted by the neighbouring nitrogen. High yields and satisfactory diastereoselectivities are always achieved.

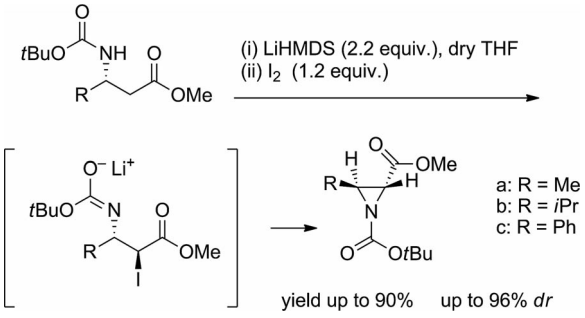

Scheme 1. General method for the synthesis of 3-alkyl/aryl-substituted *N*-Boc-2-carboxymethylaziridines.

Catalysis with Brønsted acids has been reported in the past,[18] but affords complex mixtures of products. Treatment of *N*-Boc-2-carboxymethylaziridines with $BF_3{\cdot}Et_2O$ or $BF_3{\cdot}2H_2O$ affords the corresponding 4-carboxymethyloxazolidin-2-ones in poor yields. In contrast, very good results are obtained when the reactions are performed in the presence of catalytic amounts of chelating Lewis acids,[19] such as $Cu(OTf)_2$, $Sn(OTf)_2$ and $Zn(OTf)_2$.

The rearrangements proceed with complete regio- and stereoselectivity, with the oxygen always migrating away from the carboxymethyl group. Moreover, the rearrangements are totally stereoselective, with *cis*- and *trans*-disubstituted *N*-Boc-aziridines affording exclusively *cis*- and *trans*-oxazolidin-2-ones, respectively. This behaviour can be explained by analysing the probable reaction mechanism, shown in Scheme 2. The Lewis acid catalyses the formation of an incipient carbocation on C3, which is the driving force for the rearrangement that proceeds with the elimination of a molecule of isobutene.

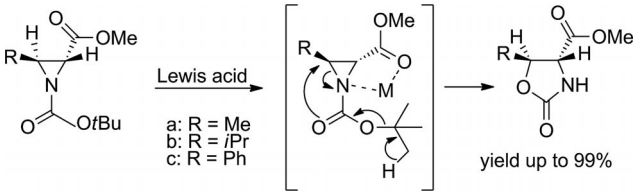

Scheme 2. General method for rearrangements of *N*-Boc-2-carboxymethylaziridines.

1.1.1. Preparation of Other Carboxyoxazolidin-2-ones

Benzyl (4*R*,5*S*)-4-{[*tert*-butyl(dimethyl)silyl]oxymethyl}-2-oxooxazolidine-5-carboxylate (**A**) and benzyl (4*S*,5*S*)-5-{[*tert*-butyl(dimethyl)silyl]oxymethyl}-2-oxooxazolidine-4-carboxylate (**B**) can be obtained in a similar way from L-aspartic acid (Figure 2).[20]

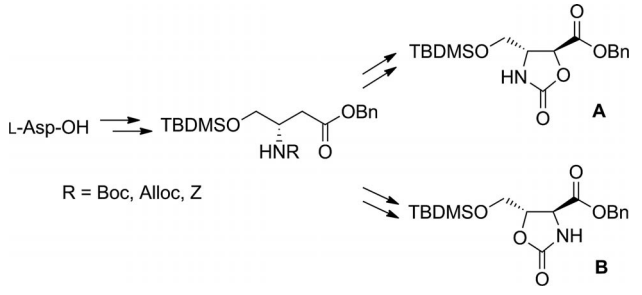

Figure 2. Synthetic scheme for the preparation of the the regioisomeric oxazolidin-2-ones **A** and **B** from L-aspartic acid.

The common reagent for the highly stereoselective synthesis of the two compounds was a fully protected β-amino-γ-hydroxybutanoic acid, obtained in five steps from commercially available Z-Asp-OH (Z = carbobenzoxy) or Boc-L-Asp-OH (Boc = *tert*-butoxycarbonyl). Alloc-L-Asp-OH (Alloc = allyloxycarbonyl) was prepared from L-Asp-OH and AllocCl in dimethyl formamide (DMF) in the presence of diisopropyl ethyl amine (DIEA).[21]

The introduction of the stereogenic centre at C2 was achieved by formation of the corresponding lithium salt and quenching with iodine with the formation of the corresponding aziridines (Scheme 3). The oxazolidin-2-one was prepared by ring-expansion of the carboxyaziridine, catalysed by $Sn(OTf)_2$; the reaction is totally regio- and diastereoselective. The presence of an azaphilic Lewis acid, such as $Sn(OTf)_2$, promotes the rearrangement, which is enhanced and directed by the presence of the adjacent carboxy group, whereas the *tert*-butyldimethylsilyloxy group does not affect the regioselectivity.

Moreover, the corresponding reaction in dry toluene resulted in the exclusive formation of the corresponding *anti* α-iodo derivative,[22] which can be isolated as a single stereoisomer and transformed into the *trans*-oxazolidin-2-one in quantitative yield simply by treatment with microwaves in DMF (Scheme 4). This alternative method therefore allows us to prepare the regioisomer of the previously prepared compound.

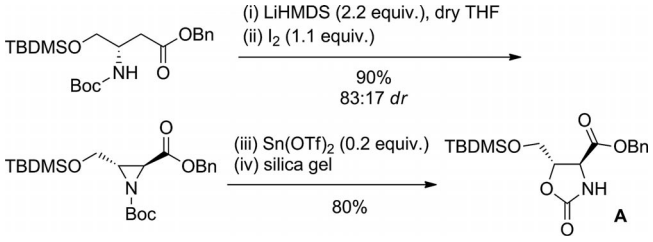

Scheme 3. Synthesis of benzyl (4*S*,5*S*)-5-{[*tert*-butyl(dimethyl)silyl]-oxymethyl}-2-oxo-oxazolidine-4-carboxylate (**A**).

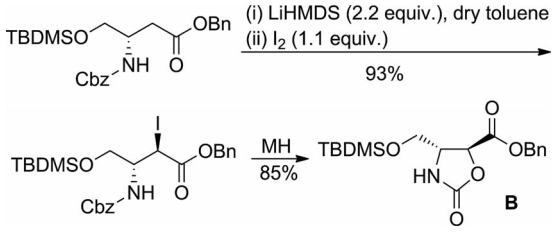

Scheme 4. Synthesis of (4*S*,5*S*)-5-{[*tert*-butyl(dimethyl)silyl]oxymethyl}-2-oxooxazolidine-4-carboxylate (**B**).

1.2. Preparation of 2-[(4*S*)-2-oxooxazolidin-4-yl]acetate (D-Oxac)

A couple of syntheses of 2-[(4*S*)-2-oxooxazolidin-4-yl]-acetate (D-Oxac) derivatives have been described;[23] they are based on hydrolysis or alcoholysis of (3*S*)-[(carbobenzyloxy)amino]-γ-butyrolactone, prepared in turn from Z-L-Asp-OH by a known procedure.[24] The benzyl ester D-Oxac-OBn can be efficiently synthesized from Z-L-Asp-OH in a four-step preparation (Scheme 5).[25] On treatment with neat Ac_2O under microwave irradiation conditions, Z-L-Asp-OH was transformed into the corresponding anhydride, which was reduced with $NaBH_4$ to a mixture of lactone and hydroxyacid. This mixture was treated with Cs_2CO_3 to provide (quantitative yield) the caesium carboxylate, which was transformed into the benzyl ester and purified.

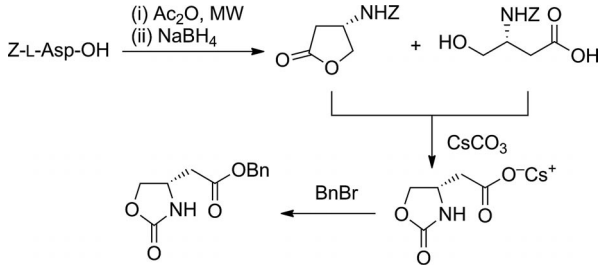

Scheme 5. Synthesis of 2-[(4*S*)-2-oxooxazolidin-4-yl]acetate (D-Oxac).

1.3.Preparation of Imidazolidin-2-one-4-carboxylates (Imz)

The Hofmann rearrangement is a well-known reaction that easily allows the transformation of primary amides into amines[26] by treatment with bromine under aqueous basic conditions. Several methods employing different reagents that are generally able to deliver a positive halogen have been described.[27] However, the classical method for converting a primary carboxamide into an amine with the aid of an alkaline solution of bromine can be unsatisfactory and unreliable.[28]

This method allows imidazolidin-2-one-4-carboxylate (Imz) and 2-(tetrahydro)pyrimidin-2-one-5-carboxylate to be obtained on multigram scales[29] through the rearrangements of protected asparagine (Asn) and glutamine (Gln) derivatives, respectively, in the presence of $PhI(OAc)_2$[30] (Scheme 6).

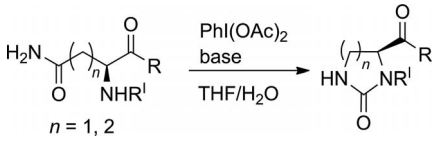

Scheme 6. General method for rearrangements of protected asparagine or glutamine derivatives.

THF is the solvent of choice for these reactions under any conditions. 1,8-Diazabicyclo[5.4.0]undec-7-ene (DBU) is needed for the formation of five-membered rings, whereas for the formation of the six-membered rings better results were obtained with DIEA.

The most likely reaction mechanism follows a path similar to that of the classical Hofmann rearrangement.[31] The first step is the formation of an intermediate (Figure 3) that easily evolves into the corresponding isocyanate. This in turn is trapped by the nitrogen of the carbamate (or amide) unit, thus forming a five- or six-membered ring in a thermodynamically driven process.

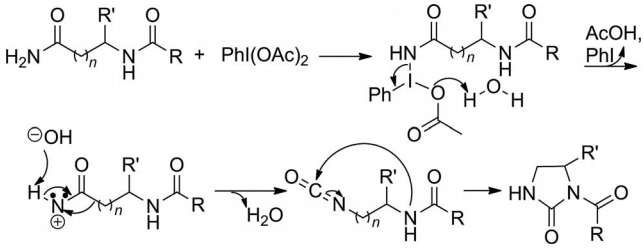

Figure 3. Reaction pathway for the formation of 2-oxaimidazolidinones (n = 1) or of 2-(tetrahydro)pyrimidinones (n = 2).

1.4. Acylation of Oxazolidin-2-ones and Related Molecules

γ-Lactams, oxazolidin-2-ones and imidazoldin-2-ones each contain a nitrogen that is a poor nucleophile, relative to the proline amino group. The acylation procedures therefore require some attention and are discussed here.

1.4.1. Acylation of the Pyroglutamic Acid Moiety (pGlu)

The acylation of *p*Glu-OBn was performed with *N*-protected amino acids in which the acidic moieties had been transformed into the corresponding pentafluorophenyl esters.[32] The coupling with *p*Glu-OBn was performed in the

presence of several bases under inert atmosphere (Scheme 7), but very poor yields were obtained in many cases. In contrast, good to excellent results were obtained with LiHMDS, which turned out to be the reagent of choice.[33]

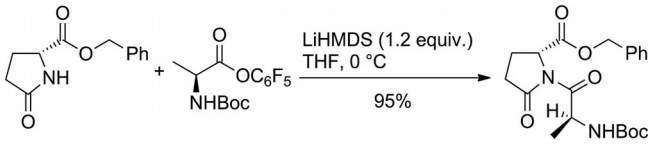

Scheme 7. General procedure for the acylation of *p*Glu-OBn.

1.4.2. Acylation of the Oxazolidinone Moiety (Oxd) for the Synthesis of Homo-oligomers

The acylation of oxazolidin-2-one moieties proved easier and the presence of a lithium base was not required. Indeed, two molecules of L-Oxd were coupled by activation of the carboxy group.[34] Previously the acylation had been performed by treatment of the carboxyl group with oxalyl chloride and DMF,[35] but this approach damages the heterocycle component. The desired Boc-L-Oxd-L-Oxd-OBn was thus obtained in quantitative yield in the presence of DIEA and a catalytic amount of dimethylaminopyridine (DMAP) in DMF. The yield is around 70%, but it is very sensitive to reaction conditions and can drop to about 30% if the reaction is not carried out carefully (Scheme 8).

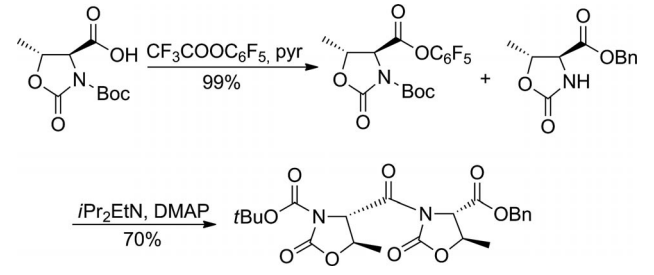

Scheme 8. Synthesis of Boc-L-Oxd-L-Oxd-OBn.

1.4.3. Acylation of the Oxazolidinone Moiety (Oxd) with Acyclic Amino Acids

Also in this case the acylation proved easier. Boc-L-Ala-L-Oxd-OBn, for instance, was obtained by coupling Boc-L-Ala-OH with H-L-Oxd-OBn in the presence of *N*-[(1*H*-benzotriazolyl)(dimethylamino)methylene]-*N*-methylmethaneiminium hexafluorophosphate *N*-oxide (HBTU)[36] and DBU in dry acetonitrile (Scheme 9). It is crucial to perform the reaction under nitrogen, because the yield falls drastically in the presence of air. Depending on the reaction conditions, HATU [2-(7-aza-1*H*-benzotriazol-1-yl)-1,1,3,3-tetramethyluronium hexafluorophosphate] or HCTU [2-(6-chloro-1*H*-benzotriazol-1-yl)-1,1,3,3-tetramethylaminium hexafluorophosphate] can be employed as coupling agents and DIEA or TEA (triethylamine) can be utilized as bases.

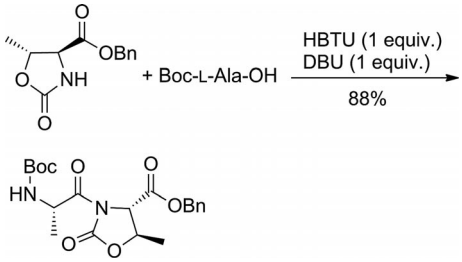

Scheme 9. General procedure for the acylation of D-Oxd.

1.4.4. Acylation of the Imidazolidin-2-one Moiety (Imz)

Direct acylation of the heterocycle nitrogen in good yield failed, so the dipeptide Boc-L-Phe-D-Imz-OBn was prepared by starting from the readily available Boc-L-Phe-D-Asn-OBn and use of the modified methodology for the Hofmann rearrangement described above (Scheme 10). After preparation and purification by conventional methods, Boc-L-Phe-D-Asn-OBn was treated with $PhI(OAc)_2$ and DBU in tetrahydrofuran (THF).

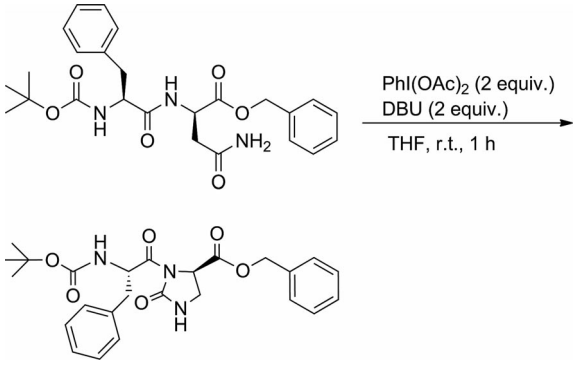

Scheme 10. Synthesis of Boc-L-Phe-D-Imz-OBn.

1.5. Synthesis of Cyclic Systems Containing Oxazolidin-2-one Units

Cyclic peptides have been extensively studied because they provide ideal scaffolds for exploring structure–activity relationships in ligand–receptor interactions.[37] Cyclization favours the mimicking of turns and the formation of intramolecular hydrogen bonds and increases membrane permeability, by eliminating charged termini.[38] Furthermore, several azole-based cyclic peptides have been isolated from marine organisms, fungi and algae: they display interesting antitumour and antidrug resistance properties and are potential metal ion chelators.[39] Cyclic pseudopeptides containing heterocycles are thus good candidates to mimic the shapes and the pharmacological activities of these interesting natural products.

Six cyclopeptide analogues of different shapes, each containing the D-Oxd unit alternating with a generic L-amino acid, have been prepared.[40] The general formula is *cyclo*-(L-AA-D-Oxd)$_n$ (where AA is a generic α-amino acid and n = 3, 4). The preparations and cyclizations of the linear pseudopeptides were performed in the liquid phase and

were compatible with different macrocycle sizes (n = 3, 4) and with several side chains, such as the fluorescent dansyl (dansyl = DANS = 5-dimethylamino-1-naphthalenesulfonyl) unit,[41] which can be used to determine the location of a molecule in a biological environment (Figure 4).[42] The best reaction conditions for cyclization were found to be with HATU and TEA as reagents in solution (5 mM) in dry acetonitrile at room temperature.

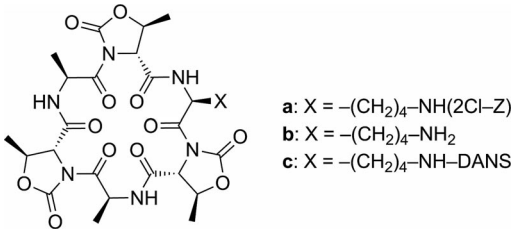

Figure 4. Chemical structures of the Oxd-containing cyclic pseudopeptides with n = 3.

2. Conformational Analysis of Foldamers Containing Oxazolidin-2-ones and Related Molecules in Solution

2.1. Conformational Analysis of Homo-oligomers in Solution

2.1.1. Homo-oligomers of L-Pyroglutamic Acid (L-pGlu)

A detailed conformation analysis of the homo-oligomers of L-*p*Glu (from monomer to tetramer, Figure 5) in solution, performed by FTIR absorption, ^{1}H NMR and CD techniques, is reported, together with the results of the crystal-state analysis by X-ray diffraction and of a high-level DFT computational modelling of Boc-(L-*p*Glu)$_2$-OH, which demonstrate that a stabilizing αC–H···O=C intramolecular H-bond is present.[43]

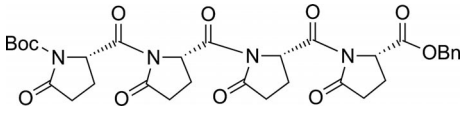

Figure 5. Chemical structure of the longest investigated L-*p*Glu homo-oligomer.

The oligomers were prepared by the coupling method described in Section 1.4.1.

From literature data on imides[44] and from comparison of the FTIR absorption spectra of the oligomers, it may be concluded that there is no evidence of any abrupt change in conformation in $CDCl_3$ solution as the pseudopeptide main chain elongates. In this pseudopeptide series the only potentially informative protons for NMR-based conformation analysis are the αCH protons. The chemical shifts of all of the αCH protons, except for those assigned to the C-terminal residues, cluster in a region significantly downfield from that common to peptide αCH protons (about 4.5–5.0 ppm):[45] this unusual shift is due to the presence of the γ-lactam carbonyl group in the vicinities of the N-terminal and internal αCH protons and is clearly absent in the case of the C-terminal αCH proton, which therefore resonates in the expected spectral region. An additional interesting piece of information extracted from this analysis is that, if the αCH proton of a given residue is close to the γ-lactam carbonyl group of the following L-*p*Glu residue, then the –CO–N< bond external to the ring system is forced to adopt the *trans* conformation. This result is not surprising on energetic grounds because this imide conformation[46] is the one that allows the two nonbonded carbonyl oxygen atoms of this semicyclic system to be located furthest apart. The conformational conclusions extracted from this NMR study fit nicely with those obtained from our FTIR absorption analysis and discussed above.

The electronic absorption spectra of the semicyclic imides Boc-(L-*p*Glu)$_n$–OH (n = 1–4) in MeOH solution (Figure 6) are each characterized by two moderately intense (ε = 4000–2000) transitions in the 200–250 nm region centred at about 210 and 220 nm.[47] Whereas the monomer exhibits a single, positive band (at 215 nm) above 200 nm, the CD spectra of the higher oligomers show dichroic doublets (positive at longer wavelengths) of regularly increasing intensity with increasing backbone length. In these three spectra the positive lobe is lower in intensity than the negative lobe and the cross-over point is at 223–225 nm. The shape similarity and the regularly increasing intensity of the CD spectra with main-chain elongation from dimer to tetramer therefore indicate the persistence of the same backbone conformation for these pseudopeptide oligomers in MeOH solution.

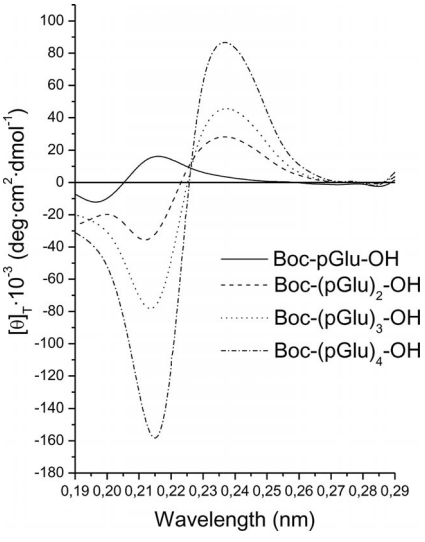

Figure 6. CD spectra of the Boc-(L-*p*Glu)$_n$-OH (n = 1–4) series in MeOH solution (conc. 1 mM).

The molecular structure of Boc-(L-*p*Glu)$_2$-OH in the crystal structure, as obtained by X-ray diffraction analysis, is shown in Figure 7. The ϕ and ψ backbone torsion angles for the two residues 1 and 2 [ϕ_1 = –58.1(6)°, ψ_1 = 146.1(4)°;

ϕ_2 = –83.2(5)°, ψ_2 = 166.8(4)°] indicate a partially extended conformation, similar to the type-II poly(-L-Pro)$_n$ structure.[48]

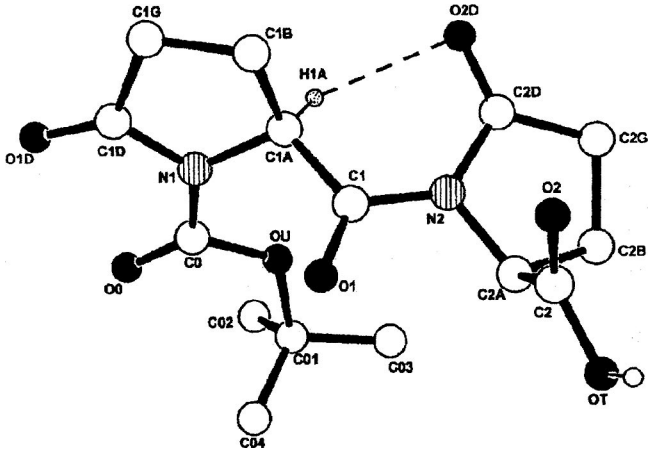

Figure 7. X-ray diffraction structure of Boc-(L-*p*Glu)$_2$-OH. Reproduced from ref.[43]

Through high-level DFT computational results for Boc-(L-*p*Glu)$_2$-OH, the occurrence of an unconventional, weak C–H···O=C H-bond interaction was investigated, this having already been recognized as a significant structural feature both in natural and in synthetic molecules.[49] The calculation results yield a ca. 1.4 kcal mol^{-1} stabilization energy due to the C1A–H1A···O2D–C2D H-bond, which is within the range reported in the literature for unconventional C–H···O=C interactions of this kind (less than 2.0 kcal mol^{-1}). The results of these calculations indicate that this weak H1A···O2D interaction also has an effect on the ^{1}H NMR spectra, in excellent agreement with the experimentally observed values.

The (L-*p*Glu)$_n$ homo-oligomers thus represent a new type of helical structure, similar to that adopted by poly-(L-Pro)$_n$ with *trans* tertiary peptide bonds (type II). Both repeating systems generate left-handed, ternary (3_1 symmetry) helices, but the (L-*p*Glu)$_n$ system is rigid and the (L-Pro)$_n$ system significantly more flexible, due to the *cis*/*trans* isomerism about the tertiary amide bonds. Because this phenomenon, particularly significant in short homo-oligomers,[50] is responsible for the onset of multiple, coexisting conformers, it is clear that the (L-Pro)$_n$ oligopeptides cannot be safely exploited as spacers or templates with reliably predetermined separations.

2.1.2. Homo-oligomers of trans-(4S,5R)-4-Carboxybenzyl-5-methyloxazolidin-2-one (L-Oxd)

Solution conformation analysis of L-Oxd homo-oligomers by FTIR absorption, ^{1}H NMR and CD techniques is discussed here. These compounds were obtained after synthesis of L-Oxd (Section 1.1) and coupling of the monomeric units (Section 1.4.2.) up to the pentamer level.[51]

From the FTIR absorption spectra of the oligomer series, it is evident that the major contribution to all four bands in the 1830–1700 cm^{-1} region is by the carbonyl stretching absorptions of the acylurethane moiety. In particular, the intensities of the two bands near 1790 and 1720 cm^{-1} regularly increase with oligomer backbone lengthening. From this FTIR absorption analysis it may be concluded that in $CDCl_3$ solution there is no evidence of any abrupt change in conformation as the pseudopeptide main chain elongates, as already observed for the L-*p*Glu series (Section 2.1.1.).

In this Boc/OBn-protected L-Oxd series the only potentially informative protons for a ^{1}H NMR conformation analysis are the αCH protons. As discussed for the L-*p*Glu series in Section 2.1.1., the chemical shifts of all αCH protons in $CDCl_3$ solution, except for that assigned to the C-terminal residue, cluster in a region significantly downfield from that common to peptide αCH protons (about 4.5–5.0 ppm) and especially to the αCH protons of poly (L-Pro)$_n$ II (δ =4.80 ppm).[52] This unusual shift is due to the presence of an oxazolidin-2-one carbonyl in the vicinity of the N-terminal and internal αCH protons. This αC–H···O=C interaction is clearly absent in the case of the C-terminal αCH proton, which therefore resonates in the expected spectral region.

The CD spectra series suggests conclusions similar to those observed for the L-*p*Glu series. Whereas the monomer exhibits a single, weak and positive band (at about 215 nm) above 200 nm, the CD spectra of the higher oligomers show dichroic doublets of regularly increasing intensity with increasing backbone length. In these spectra the positive lobes are lower in intensity than the negative lobes and the cross-over points are at 212–216 nm. Also, these curves give rise to a nearly isodichroic point in the vicinity of 217 nm.

To determine the conformational minima for the L-(Oxd)$_n$ oligomers and to provide a more accurate explanation of their magnetic properties, fully unconstrained DFT optimizations for Boc-(L-Oxd)$_n$-OBn (n = 2–5) were carried out.

For Boc-(L-Oxd)$_2$-OBn, the fully relaxed structure does seem to involve an αC–H···O=C interaction as shown for the related (L-pGlu)$_2$ oligomer. To validate the optimized structure further, the ^{1}H NMR chemical shift (δ) values for its CHα protons were simulated and compared with those observed in $CDCl_3$ solution. Although consistently shifted to higher field by about 0.4 ppm (this effect is due to the approximation of the simulation method used here),[53] the simulated values for the H1A and H2A chemical shifts (δ = 4.22 ppm and δ = 5.12 ppm, respectively) do in fact exhibit the same trend as the experimental data. In conclusion, the anomalous downfield chemical shift both computed and observed for the proton H1A can be ascribed to the noncovalent H1A···O2D interaction. The strength of such a weak αCH···O=C interaction was judged to be about 1.5 kcal mol^{-1}, as previously reported.

The lowest energy minimum for trimer, tetramer and pentamer was optimized in a similar fashion, thus showing that for each homo-oligomer there are n – 1 (where n is the number of monomers in each molecule) downfield-shifted protons and, as a consequence, that there are also n – 1 αC–H···O=C hydrogen bonds. These interactions, although

weak, do stabilize the overall secondary structure, allowing the molecule to adopt a robust poly (L-Pro)$_n$ II-type helix (3_1 helix) (Figure 8).

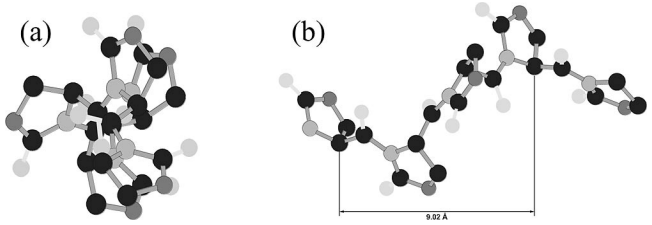

Figure 8. (a) Front view and (b) side view of the calculated Boc-(L-Oxd)$_5$-OBn helix. The terminal protecting groups have been removed. Reproduced from ref.[51]

2.1.3. Homo-oligomers of (4R)-(2-Oxo-1,3-oxazolidin-4-yl)-acetic Acid (D-Oxac)

The homo-oligomers of D-Oxac (a cyclic β-amino acid derivative) would be expected to adopt more flexible structures than those characteristic of their α-amino acid counterparts, although they still contain imide moieties (Figure 9).[54]

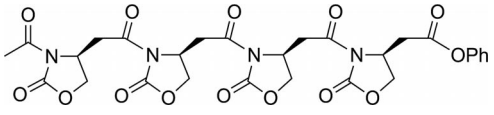

Figure 9. Chemical structure of the longest D-Oxac homo-oligomer investigated.

The synthesis of the homo-oligomers was achieved under liquid-phase conditions by the previously described procedure (Section 1.4.2). With formation of the longer oligomers the compounds become progressively more water-soluble.

An experimental investigation of the preferred conformation assumed by Ac-(D-Oxac)$_n$-OBn (n = 1–4) oligomers in $CDCl_3$ solution was performed by ^{1}H NMR spectroscopy. The chemical shifts of the α-protons of the four oligomers are more deshielded by about 0.5 ppm relative to those of the C-terminal ring, which resonate in the expected spectral region. This has previously been observed in all of the pseudopeptides containing oxazolidin-2-ones or γ-lactam rings (Section 2.1.1. and 2.1.2.) and is due to the presence of an endocyclic carbonyl in close proximity to the αCH protons, so it is a general effect. A similar effect has also been observed for the β-protons, but in this case it is much weaker, with a variation of only about 0.1 ppm found. Because both the α- and the β-protons of each D-Oxac oligomer are affected by the presence of the endocyclic carbonyl, a reasonable preferred conformation should invoke an *anti* disposition for the two carbonyls.

With the aim of confirming these experimental results and in particular of obtaining a better insight into the conformational preference of the Ac/OBn D-Oxac tetramer both in a solvent that would support a 3D structure (chloroform) and also in a competitive solvent (water), an extensive unconstrained conformation analysis was performed by varying all of the degrees of freedom with use of the Monte Carlo[55] conformational search (MC/EM), the OPLS* force field[56] for energy calculation and the GB/SA both in water and chloroform to include the solvent effect.[57]

Different results were obtained upon switching the analysis from structure-supporting solvents (e.g., chloroform) to competitive solvents (e.g., water). Nevertheless, all of the conformations, both in water and in chloroform, show an *anti* orientation for the two carbonyl groups of each imide moiety. Furthermore the conformation analysis clearly showed this molecule folding in an ordered helix in competitive solvents such as water. This outcome was validated by DFT ^{1}H and ^{13}C NMR simulations that furnished chemical shifts that matched the experimentally measured values. Because the water environment is of major importance in biological systems, the molecules described in this paper are good candidates for biological application.

2.2. Conformational Analysis of Alternated Hybrid Oligomers in Solution

2.2.1. Oligomers of the Boc-(Gly-L-Oxd)$_n$-OBn Series

The simplest oligomers that can be prepared have the general formula Boc-(Gly-L-Oxd)$_n$-OBn (Gly = glycine).[58] The synthetic approach used to prepare the Boc-(Gly-L-Oxd)$_n$-OBn units (n = 1–4; cf. Figure 10) has already been described in Section 1.4.3.

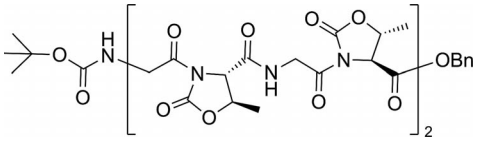

Figure 10. Chemical structure of the longest investigated Boc-(Gly-L-Oxd)$_n$-OBn oligomer.

In order to establish whether these molecules were foldamers, their behaviour was analysed by IR, CD and ^{1}H NMR spectroscopy.

From the IR absorption spectra of all the synthesized molecules (3 mM solutions in dichloromethane) there is a continuous shift of the NH stretching bands from n = 1 (no tendency to form a C=O···H–N hydrogen bond) to n = 4 (band at 3395 cm^{-1}), thus suggesting the existence of a cooperative effect.

To validate these results further, the oligomers were analysed by ^{1}H NMR spectroscopy: the $CH_2\alpha$ signals are all more deshielded, by about 0.5–0.6 ppm, than the Boc-Gly-L-Pro-NHMe α-protons. Even in the longer oligomers, with complex ^{1}H NMR spectra, all the $CH_2\alpha$ signals are between 4.20 and 4.80 ppm, thus confirming that all the imide groups assume a preferential conformation with the two carbonyls in a *trans* relationship, as expected, even with the small glycine unit.

The regular increase in C=O···H–N hydrogen bonds from n = 1 to n = 4 suggested by the IR analysis was also detected on investigation of the [D_6]DMSO dependence of the NH proton chemical shift.[59] Whereas the variation of

chemical shift with increasing [D$_6$]DMSO percentage is very large for Boc-(Gly-L-Oxd)$_2$-OBn, the titration of Boc-(Gly-L-Oxd)$_4$-OBn results only in a small variation of the chemical shift of the NH units, in good agreement with the IR of the NH region, thus suggesting that a secondary structure is formed in the longer chain.

Finally, the per-residue CD signals change on going from n = 1 to n = 4 with a dramatic increase in absorbance, thus showing that an extra effect besides the chromophore absorption is present. This can be attributed to the formation of hydrogen bonds and, as a result, of a secondary structure. This outcome is perfectly in agreement with the analysis of the IR and ^{1}H NMR spectra, which furnished evidence for the formation of hydrogen bonds.

2.2.2. Oligomers of the Boc-(L-Ala-L-Oxd)$_n$-OBn and Boc-(L-Ala-D-Oxd)$_n$-OBn Series

To investigate the preferred conformations of oligomers of the Boc-(AA-Oxd)$_n$-OBn series further, Gly was replaced with Ala, thus introducing a methyl group as a side chain (Figure 11).[60] Very probably, the methyl group should be introduced only on one face of the Gly methylene moiety, because only one side would be expected to afford a stable secondary structure, whereas the other might obstruct helix formation. Oligomers of both the Boc-(L-Ala-L-Oxd)$_n$-OBn (Ala = alanine) and the Boc-(L-Ala-D-Oxd)$_n$-OBn series were therefore synthesized, in order to check whether the Gly pro-*S* hydrogen or the pro-*R* hydrogen should be replaced. Furthermore, both hydrogen atoms were substituted in more constrained oligomers in which Gly was replaced with Aib (Aib = 2-aminoisobutyric acid).[61]

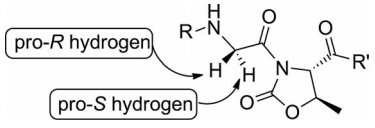

Figure 11. Chemical structure of the segment R-Gly-L-Oxd-R′. The *pro-R* and the *pro-S* α-hydrogen atoms in the Gly residue are highlighted.

The pseudopeptide chains were prepared in the liquid phase, starting from H-L-Oxd-OBn, H-D-Oxd-OBn, Boc-L-Ala-OH and Boc-Aib-OH, by the previously reported methods (Section 1.4.3.).

The L-Ala-L-Oxd oligomers were prepared up to the tetramer level (Figure 12), because of the low solubilities of the products. This effect usually indicates that the compound has a high tendency to self-aggregate.

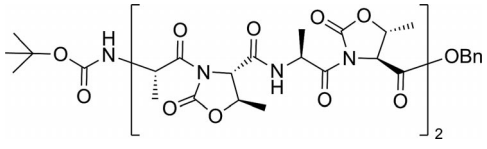

Figure 12. Chemical structure of the longest Boc-(L-Ala-L-Oxd)$_n$-OBn species investigated.

The oligomers of the Boc-(L-Ala-D-Oxd)$_n$-OBn series were then prepared by the same synthetic strategy. Luckily, the compounds of this series proved to be more soluble in organic solvents, so we could easily make Boc-(L-Ala-D-Oxd)$_6$-OBn (Figure 13).

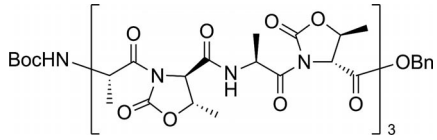

Figure 13. Chemical structure of the longest Boc-(L-Ala-D-Oxd)$_n$-OBn species investigated.

In the Aib-Oxd series, only Boc-(Aib-L-Oxd)$_2$-OBn and Boc-Aib-L-Oxd-Aib-D-Oxd-OBn were prepared, because of the low reactivity of the hindered Aib α-amino group.

Information on the preferred conformations of the described oligomers in solution was obtained in structure-supporting solvents (dichloromethane, deuteriochloroform and methanol) by FTIR absorption, ^{1}H NMR and CD techniques. Three sets of oligomers were analysed: (i) **A**: Boc-(L-Ala-L-Oxd)$_n$-OR with n = 1–4 (R = Bn, H), (ii) **B**: Boc-(L-Ala-D-Oxd)$_n$-OR with n = 1–6 (R = Bn, H), (iii) **C**: Boc-(Aib-L-Oxd)$_n$-OR with n = 1–2 and Boc-Aib-L-Oxd-Aib-D-Oxd-OR (R = Bn, H). The FTIR absorption spectra of the three sets (3 mM solutions in dichloromethane) were obtained: the results show that the three series behave in very different ways. Indeed, the compounds of the **A** and the **C** sets show no propensity to form intramolecular C=O···H–N hydrogen bonds, whereas those of the **B** set form strong hydrogen bonds in oligomers longer than the trimer.

To validate these results further, the three sets of oligomers were analysed by ^{1}H NMR spectroscopy, because the formation of a C_{i+1}=O···H–C_i intramolecular H-bond can be spotted simply by checking the chemical shift of the α-proton, because the carbonyl proximity involves a marked deshielding of the proton. In these series we observed this effect only in the L-Ala-containing sets **A** and **B**, because the Aib residues of set **C** have no α-hydrogen atoms.

Interestingly, the oligomers of both the **A** and the **B** sets follow this trend, regardless of the absolute configurations of carbons 4 and 5 of the Oxd moiety, which in contrast are crucial for the formation of intramolecular O=C···H–N hydrogen bonds, as deduced by IR absorption spectra analysis.

Although the oligomers of the **C** set do not contain α-protons capable of forming C=O···H–C$^\alpha$ H-bonds, the two nonbonded carbonyl oxygen atoms of each semi-cyclic system are still located as far apart as possible. This outcome was fully demonstrated by an X-ray diffraction analysis carried out on a single crystal of Boc-Aib-L-Oxd-OBn.

The occurrence of intramolecular C=O···H–N H-bonds in oligomers of the **A** and **B** sets was further determined by investigation of the [D$_6$]DMSO dependence of the NH proton chemical shifts. The outcome of these titrations is in perfect agreement with the results obtained from FTIR absorption: the NH protons of Boc-(L-Ala-L-Oxd)$_3$-OBn are very sensitive to DMSO, and so it is unable to form an H-

bond-driven secondary structure [Boc-(L-Ala-L-Oxd)$_4$-OBn was not analysed, owing to its poor solubility], whereas all of the NH protons of Boc-(L-Ala-D-Oxd)$_4$-OBn and Boc-(L-Ala-D-Oxd)$_5$-OBn are almost insensitive to DMSO.

Another interesting piece of information was obtained in ROESY experiments with a solution (10 mM) of Boc-(L-Ala-D-Oxd)$_5$-OBn in $CDCl_3$. From an inspection of the area between δ = 7 and 9 ppm, many $N_iH \rightarrow N_{i+1}H$ cross peaks, which usually represent the formation of an helix, are visible.[62]

Further confirmation of helix formation in the longer oligomers of the **B** set was obtained by recording the CD spectra of all the free acids of sets **A**–**C** in MeOH solution.[63] The per-residue CD spectra of the **A** and **C** sets (not shown) do not exhibit any significant change from the monomers to the higher oligomers, thus showing that no configuration-based effects take place.

The per-residue CD spectra of the **B** set are shown in Figure 14. Ellipticity increases, associated with reversal of the Cotton effect, were observed for Boc-(L-Ala-D-Oxd)$_5$-OH and, more dramatically, for Boc-(L-Ala-D-Oxd)$_6$-OH, thus suggesting the formation of ordered secondary structures. To define their natures, the CD spectrum of Boc-(L-Ala-D-Oxd)$_6$-OH, recorded at different concentrations (not shown), does not show any change as the concentration decreases: this finding excludes formation of self-associated secondary structures.

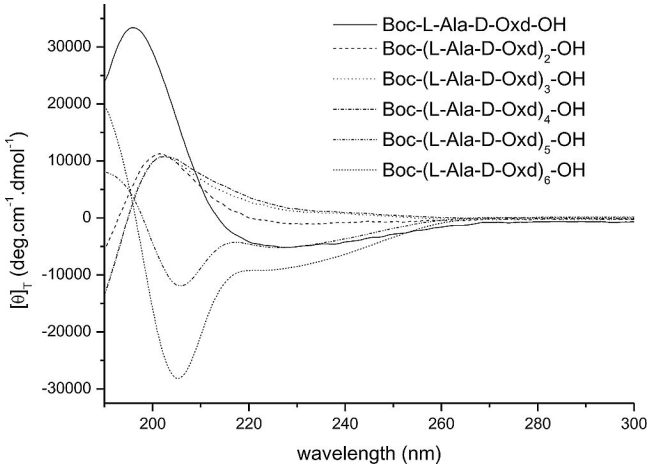

Figure 14. Normalized per-residue CD spectra of Boc-(L-Ala-D-Oxd)$_n$-OH (n = 1–6, 1 mM in MeOH).

Of the ordered peptide secondary structures that could be formed, the CD spectra of the α and 3_{10} helixes and the β pleated sheet conformations were considered. From a general inspection of the spectra shown in Figure 14, Boc-(L-Ala-D-Oxd)$_5$-OH and Boc-(L-Ala-D-Oxd)$_6$-OH clearly fold in the 3_{10} helix configuration. Indeed, Toniolo and coworkers[64] demonstrated that a 3_{10} helix can be assigned by its CD spectrum, in agreement with theoretical calculations.[65] Both theoretical and experimental studies point to the following main characteristics of the 3_{10} helix: a) a negative CD band centred near 207 nm, b) a negative shoulder in the vicinity of 222 nm, c) a $R = [\theta]_{222}/[\theta]_{207}$ ratio much weaker than the value reported for the α-helical peptides, which usually exhibit R values of about 1, and d) a positive maximum at 198 nm. Our experimentally measured CD data meet all of the requirements for the 3_{10} helix. More precisely, a β bend ribbon spiral structure can be attributed to Boc-(L-Ala-D-Oxd)$_5$-OH and Boc-(L-Ala-D-Oxd)$_6$-OH.[66] It may be considered a subtype of the polypeptide 3_{10} helix, being stabilized by alternate 1←4 intramolecular C=O···H–N H-bonds and having approximately the same folding of the peptide chain.

This outcome may be ascribed to the cooperative effect of many factors: i) the rigid –CO–N(CH<)–CO– moiety, which always tends to assume a *trans* conformation, ii) the formation of C=O···H-$^{\alpha}$C H-bonds, and iii) the alternate formation of C=O···H–N H-bonds. The combination of these three effects can thus hold the oligomers in a well defined, rigid conformation (Figure 15).

With these requirements in mind, it is clear that only oligomers of the **B** set form a β bend ribbon spiral, and that the oligomers of the **A** and **C** sets do not.

2.2.3. Oligomers of the Boc-(L-Phe-D-Oxd)$_n$-OBn Series

The structures of Boc-(L-Phe-D-Oxd)$_n$-OBn (n = 2–5) were investigated both in solution and in the solid state.[67] This section discusses the preferential conformation in solution, whereas the behaviour in the solid state is discussed in Section 4.3. The longest oligomer that has been prepared is shown in Figure 16.

Information on the preferred conformations of the oligomers in solution was obtained by analysis of FTIR, ^{1}H NMR and CD absorption spectra. The FTIR spectra were recorded as 3 mM solutions in dichloromethane. For the compound Boc-(L-Phe-D-Oxd)$_2$-OBn only one band centred at 3430 cm^{-1} is observed, so it does not form intramolecular

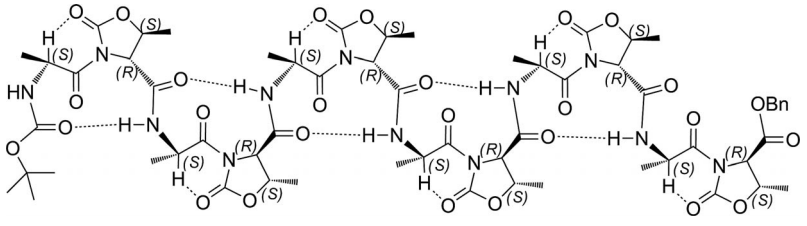

Figure 15. Conformation of Boc-(L-Ala-D-Oxd)$_6$-OBn, with the three stabilizing effects shown: (a) the rigid –CO–N(CH<)–CO– moiety, (b) the C=O···H–C H-bonds and (c) the C=O···H–N H-bonds.

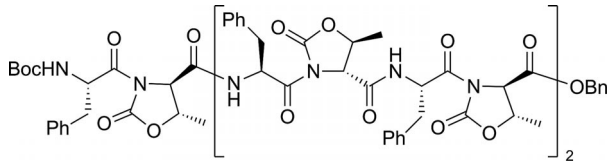

Figure 16. Chemical structure of the longest Boc-(L-Phe-D-Oxd)$_n$-OBn species investigated.

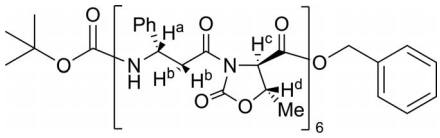

Figure 17. Chemical structure of the longest Boc-[(*S*)-β^3-hPhg-D-Oxd]$_n$-OBn species investigated.

N–H···O=C hydrogen bonds. For the compounds Boc-(L-Phe-D-Oxd)$_4$-OBn and Boc-(L-Phe-D-Oxd)$_5$-OBn a band centred at about 3280 cm^{-1} replaces it, whereas the compound Boc-(L-Phe-D-Oxd)$_3$-OBn shows both bands, so equilibria between unfolded and folded conformations result for these structures. In particular, Boc-(L-Phe-D-Oxd)$_5$-OBn shows a high tendency to form intramolecular hydrogen bonds, as indicated by the strong stretching band at 3270 cm^{-1}. A similar trend can be observed for the CO stretching bands, with the appearance of a band centred at about 1670 cm^{-1} only in the cases of Boc-(L-Phe-D-Oxd)$_4$-OBn and Boc-(L-Phe-D-Oxd)$_5$-OBn. These preliminary results suggest that at least four L-Phe-D-Oxd units are required to obtain a folded structure, as was also observed for the oligomers of the L-Ala-D-Oxd series (Section 2.2.2.).

Confirmation of the occurrence of intramolecular C=O···H–N bonds was obtained by recording ^{1}H NMR spectra of the oligomers in [D$_6$]DMSO (3 mM) at different temperatures. It is well known that in [D$_6$]DMSO the values for hydrogen-bonded amide protons are at most 4 ppb K^{-1}.[68] The variation of the chemical shifts for Boc-(L-Phe-D-Oxd)$_2$-OBn and Boc-(L-Phe-D-Oxd)$_3$-OBn are always larger than 4 ppb K^{-1}, whereas the four recorded amide and Boc protons of Boc-(L-Phe-D-Oxd)$_5$-OBn have all temperature coefficients smaller than 4 ppb K^{-1}, which is consistent with hydrogen-bonded NH protons. NOESY experiments recorded on Boc-(L-Phe-D-Oxd)$_5$-OBn confirm the conclusions drawn from the preceding experiments.

Additional information on the folding propensities of these compounds was obtained by means of ^{1}H NMR experiments in solution. Analysis of the CHα protons of the Phe units shows that the CHα chemical shifts are always around 5.5–6.0 ppm in these compounds, thus suggesting the formation of unconventional, weak CH···O=C intramolecular H-bonds.

CD spectroscopy did not provide conclusive results, due to the strong absorptions of the phenyl groups around 200 nm.[69]

In conclusion, in the higher oligomers, the tendency to form ordered secondary structures increases and seems to be fully manifested at the pentamer level.

2.2.4. Oligomers of the Boc-[(S)-β^3-hPhg-D-Oxd]$_n$-OBn Series

Novel foldamers of general formula Boc-[(*S*)-β^3-hPhg-D-Oxd]$_n$-OBn (n = 1–6) [(*S*)-β^3-hPhg = (*S*)-β^3-homophenylglycine] were synthesized in the liquid phase by the previously described methods (Figure 17).[70]

Information on the preferred conformations in solution was obtained by FTIR, ^{1}H NMR and CD techniques. The FTIR absorption spectra of all the benzyl esters (n = 1–6) suggest that the longer oligomers of this series form strong C=O···H–N hydrogen bonds, because the absorption band shifts slowly towards 3289 cm^{-1} in Boc-[(*S*)-β^3-hPhg-D-Oxd]$_6$-OBn.

For further validation of these results, the oligomers were analysed by ^{1}H NMR spectroscopy to check the formation of unconventional, weak CH···O=C intramolecular H-bonds, leading to significant deshielding of the proton chemical shifts. Indeed, the CHα hydrogen atoms of the *h*Phg units are always more deshielded, by about 0.3–0.4 ppm, than the CHα hydrogen atoms in Boc-β^3-hPhg-OH.[71]

Furthermore, the occurrence of intramolecular C=O···H–N hydrogen bonds in Boc-[(*S*)-β^3-hPhg-D-Oxd]$_6$-OBn was detected by investigation of the temperature-dependence of the NH proton chemical shifts in [D$_6$]DMSO. Whereas the five recorded amide protons have small temperature coefficients consistent with those for hydrogen-bonded NH protons (ppb K^{-1} = 3.46–3.54), the Boc-NH has a larger temperature coefficient (ppk K^{-1} = 7.51), suggesting that this proton is not involved in a hydrogen bond. This might be the result of its position at the beginning of the chain. Finally, NOESY experiments were recorded on the same compound and show the presence of cross-peaks between the NH amide hydrogen atoms (8.50–9.00 ppm) that clearly indicate helix formation.[62]

Some support for the formation of ordered secondary structures in the longer oligomers is provided by the CD spectra (Figure 18) of all the oligomers as free acids (n = 1–6) in MeOH solution. For n = 1, the CD spectrum exhibits a minimum at 193 nm and a maximum at 202 nm. The minimum slowly moves towards 196 nm in the longer oligomers with increasing intensity. The maximum at 202 nm gradually disappears and is replaced by a shoulder at 202–206 nm. When n = 6, the CD spectrum is even more different, with a minimum at 197 nm of much lower intensity and a new maximum at 220 nm. This variation suggests the formation of an ordered structure, although the CD spectra do not permit the determination of the actual nature of this structure. CD spectra of α,β-hybrid peptides have recently been reported, but no clear correlation between structured helices and CD spectra, as is known for native helices, could be established.[72]

To obtain more insight into the nature of the hydrogen-bonded secondary structure indicated by the experimental investigations, quantum chemical calculations were per-

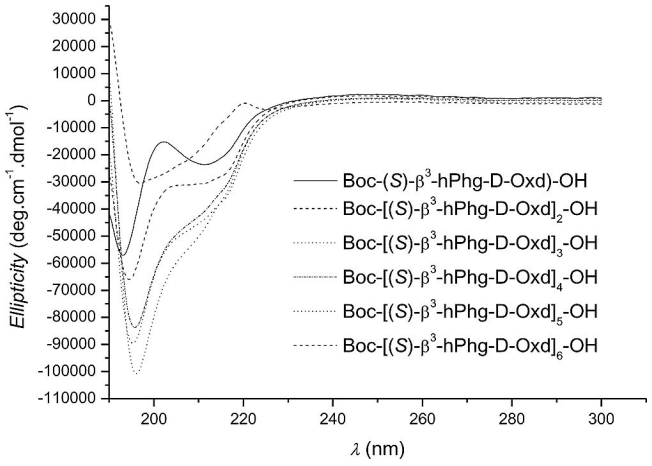

Figure 18. Normalized per-residue CD spectra (1 mM in MeOH) of Boc-[(*S*)-β^3-hPhg-D-Oxd]$_n$-OH (n = 1–6).

formed on the oligomers Boc-[(*S*)-β^3-hPhg-D-Oxd]$_3$-OBn and Boc-[(*S*)-β^3-hPhg-D-Oxd]$_6$-OBn with the aid of ab initio MO theory at the HF/6–31G* level. It was thus possible to predict all helix types that can be expected in oligomers of regular α,β-hybrid peptides. Theoretical calculations based on ab initio MO theory suggest a helix with 11-membered hydrogen-bonded rings as the preferred secondary structure type. A left-handed mixed $H_{(11)/9}$ helix was also obtained as a conformer, but it is less stable than the H_{11} hexamer and the hydrogen bond lengths are too long, because of steric effects caused by the oxazolidin-2-one rings.

3. Secondary Structures and Applications of Oxazolidin-2-ones Containing Reverse-Turn Mimics

Reverse-turns are common motifs in protein structures and account for up to one-third of the residues in globular proteins.[73] A turn can be defined as the site where the peptide changes its overall direction. Section 2 describes the conformation analysis of oxazolidin-2-one-type foldamers, demonstrating that those new polyimides behave as rigid spacers as a result of the presence of the endocyclic carbonyl group, which imparts a strictly *trans* conformation to the adjacent peptide bond.

The introduction of conformationally constrained analogues can be very useful in the de novo design of a reverse-turn conformation, so studies on imidic bond conformational behaviour have been extended to some short oligopeptides containing L-*p*Glu, L-Oxd, D-Oxd or D-Oxac moieties as residue *i*+1 and Gly or Aib as residue *i*+*2* (Figure 19).[74]

In naturally occurring reverse-turns this position is often occupied by L-Pro (Pro = proline), so the introduction of an oxazolidin-2-one moiety could favour the formation of a β-hairpin secondary structure. To study and to compare their conformational preferences, conformation analysis and DFT calculations have been performed on the most interesting molecules.

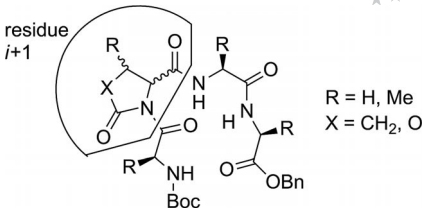

Figure 19. General structure of the fully protected tetramers.

All the compounds [Boc-L-Ala-L-pGlu-Gly-L-Ala-OBn, Boc-L-Val-L-pGlu-Gly-L-Ala-OBn, Boc-L-Val-L-pGlu-Aib-L-Ala-OBn, Boc-L-Val-L-Oxd-Gly-L-Ala-OBn, Boc-L-Val-D-Oxd-Gly-L-Ala-OBn, Boc-L-Val-D-Oxd-Aib-L-Ala-OBn, Boc-L-Val-D-Oxac-Gly-L-Ala-OBn and Boc-L-Val-D-Oxac-Aib-L-Ala-OBn (Val = valine)] were prepared by liquid-phase synthesis. Some reference compounds containing the L-Pro or D-Pro moiety were also prepared. These compounds were all analysed by IR, ^{1}H NMR and ESI-MS. The molecules containing D-Oxd show good propensities towards the formation of β hairpin conformations. Among them, the best results were obtained with Boc-L-Val-D-Oxd-Gly-L-Ala-OBn, which assumes a preferential β turn conformation in chloroform and a preferential γ turn conformation in DMSO, whereas its epimer Boc-L-Val-L-Oxd-Gly-L-Ala-OBn shows only a minor propensity to assume ordered forms. These findings were confirmed by DFT calculations, which provide an interpretation for the available experimental data and agree with the reported observations. Furthermore, the oligomers Boc-L-Val-D-Oxac-Gly-L-Ala-OBn and Boc-L-Val-D-Oxac-Aib-L-Ala-OBn also give interesting results, both showing good propensity to form a β hairpin conformation.

The LC/ESI-MS analysis demonstrate that only the tetramers containing L-pGlu, L-Oxd or D-Oxd show a strong tendency to chelate a molecule of water in the gas phase, whereas molecules containing L-Pro do not. This outcome suggests that this behaviour is maintained in the liquid phase and that oligopeptides containing these heterocycles show a significant tendency to chelate water molecules.

3.1. Reverse-Turn Mimic for Calcium Complexation

In view of these encouraging results, some small pseudopeptides each containing an Oxd moiety and having the general formula Ac-Oxx-L-Xaa-OBn were prepared to check their tendency to chelate calcium ions. Oxx is L-Oxd, D-Oxd or D-Oxac and Xaa is L-Ala, Aib, L-isovaline (L-Iva), L-α-methyl-valine [L-(αMe)Val] or L-α-methyl-norvaline [L-(αMe)Nva].[75]

All of these molecules were analysed in the absence of calcium ions by ^{1}H NMR, ^{13}C NMR and IR spectroscopy and by ESI-MS spectrometry. They assume different preferential conformations, although the tested molecules are very similar. Indeed, the L-Ala- and L-Val-containing dipeptides show no tendency to form NH···OC hydrogen bonds, whereas the dipeptides containing α,α-disubstituted amino acids tend to form NH···OC hydrogen bonds more easily.

The preferred conformations of Ac-L-Oxd-L-Ala-OBn (mostly nonchelated NH) and of Ac-L-Oxd-L-Iva-OBn (mostly chelated NH) were thus further determined by evaluation of inaccessible NH groups by ^{1}H NMR, by addition of increasing amounts of [D_6]DMSO to solutions (1 mM) in $CDCl_3$ (Figure 20). The results for Ac-L-Oxd-L-Ala-OBn and Ac-L-Oxd-L-Iva-OBn show that the NH of Ac-L-Oxd-L-Ala-OBn is very sensitive to DMSO ($\Delta\delta$ = 1.80 ppm), whereas the NH of Ac-L-Oxd-L-Iva-OBn displays a smaller variation of chemical shift ($\Delta\delta$ = 1.06 ppm), thus suggesting that this proton is at least partly hydrogen-bonded: this result is in agreement with the IR outcome and with NOESY1D experiments on solutions in $CDCl_3$ (10 mM).

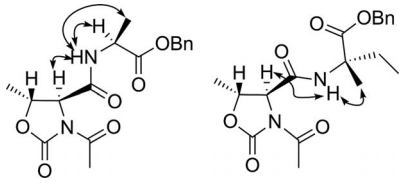

Figure 20. Preferential conformations of Ac-L-Oxd-L-Ala-OBn (left) and Ac-L-Oxd-L-Iva-OBn (right) suggested by IR and ^{1}H NMR spectroscopic data.

With regard to calcium complexation, we expect that chelation in solution would be better obtained with molecules such as Ac-L-Oxd-L-Ala-OBn, in which the Xaa carbonyl groups are already disposed in the right position. Indeed the chelation "skills" of all the dipeptides were evaluated by analysis of solutions containing protected dipeptides and calcium tetrafluoroborate (5 equiv.) with a mass spectrometer fitted with an electrospray detector (ESI-MS).

The spectra of the dipeptide + calcium ions show the characteristic presence of a [M + 20] peak, which can be attributed to an ion of formula $[2M + Ca]^{2+}$, suggesting that two molecules of dipeptide can chelate only one calcium ion, although the calcium is in large excess in the solution. Ions with formula [M + Ca], producing signals of *m*/*z* [M + 40]/2, are totally absent.

The most intense peak at [2M + Ca]/2 was observed in the ESI-MS spectrum of Ac-L-Oxd-L-Ala-OBn + Ca^{2+}. This outcome is in agreement with what we had foreseen from the study of the IR and ^{1}H NMR spectra. Figure 21 shows a possible chelation model (a hexacoordinate complex) consistent with the experimental data. Indeed this is perhaps the most common coordination number, and the six ligands almost invariably lie at the vertices of an octahedron or a distorted octahedron.[76]

Moreover, this hypothesis is also consistent with the reported cyclo-(Pro-Gly)$_3$, which forms a 2:1 complex with Ca^{2+} in which the cation is sandwiched between the two peptide molecules.[77] The Gly carbonyls from each of the peptides are octahedrally coordinated to the cation with an average calcium oxygen coordination distance of 2.26 Å.

A similar outcome, although less intense, was obtained with Ac-D-Oxd-L-Ala-OBn: this outcome shows that L-Ala moiety is very important for the receptor design, possibly

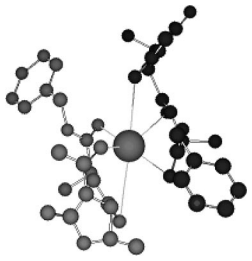

Figure 21. Hypothetical structure of the complex Ac-L-Oxd-L-Ala-OBn + Ca^{2+}, consistent with the IR, ^{1}H NMR and ESI-MS outcome. Reproduced by permission of The Royal Society of Chemistry from ref.[75]

because more hindered side chains disfavour the useful conformation for the formation of the Ca^{2+} complex.

Interestingly, the complexation process between Ac-L-Oxd-L-Ala-OBn and Ca^{2+} can also be monitored by photoluminescence spectroscopy. Figure 22 shows that a new large and unstructured bond between 400 and 600 nm appears in the emission spectrum of Ac-L-Oxd-L-Ala-OBn when Ca^{2+} (0.5 equiv.) is introduced into a solution (10^{-3} M) of Ac-L-Oxd-L-Ala-OBn in acetonitrile. On the other hand, further addition of Ca^{2+} does not induce noticeable changes in the emission spectrum. This result corroborates the hypothesis of the formation of a complex with two molecules of Ac-L-Oxd-L-Ala-OBn in which the calcium ion is hexacoordinate.

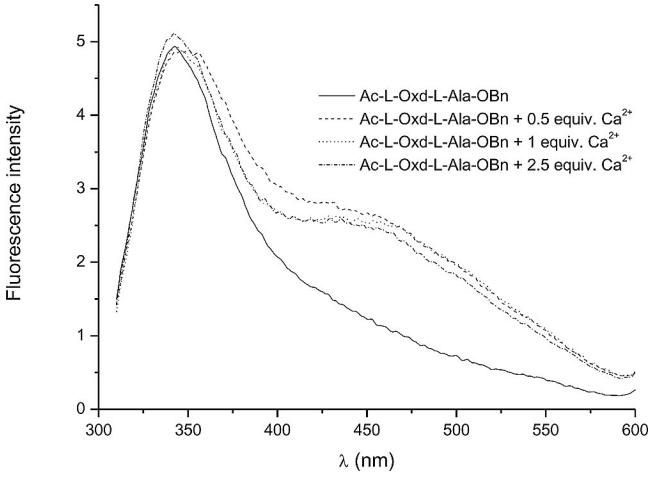

Figure 22. Fluorescence emission of Ac-L-Oxd-L-Ala-OBn in acetonitrile (1 mM). The excitation was at 285 nm.

4. Foldamers Containing Oxazolidin-2-one Units as new Supramolecular Materials

Formation of fibres through self-assembly is of particular interest, because protein fibres are involved in intra- and extracellular functions.

To understand aggregation phenomena, oligopeptides may be designed and prepared with the aims either of interfering with[78] or of mimicking these processes.[79] Indeed,

the potential applications of such supramolecular assemblies surpass those of synthetic polymers, because the building blocks might introduce biological function in addition to mechanical properties.[80]

4.1. Supramolecular Materials from Dipeptides

4.1.1. Boc-L-Phe-D-Oxd-OBn

This material was obtained as a fibre-like white solid after slow solvent evaporation of a solution of Boc-L-Phe-D-Oxd-OBn (20–25 mM) in a mixture (1:1) of cyclohexane/ethyl acetate[81] (Figure 23). The molecule also shows good solubility in polar solvents such as acetonitrile, methanol, diethyl ether and ethyl acetate, but is not soluble in water. It assembles to form a fibre-like material under a wide variety of solution conditions. This material shows strong birefringence and has defined edges. It is made of bundles of crystalline-shaped filaments clustered and aligned along the main bundle direction.

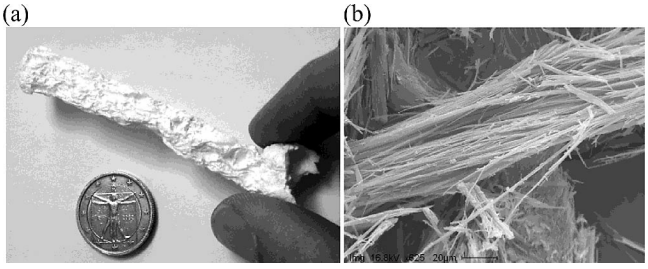

Figure 23. (a) Boc-L-Phe-D-Oxd-OBn after slow evaporation of a mixture cyclohexane/ethyl acetate (1:1). (b) SEM image of filament bundles of Boc-L-Phe-D-Oxd-OBn. Scale bar: 20 μm. Reproduced from ref.[81]

The IR spectra of Boc-L-Phe-D-Oxd-OBn in dichloromethane and of a 1% mixture of solid with KBr gave very different findings. Hydrogen bonding is clearly present in the solid, but distinctly diminished in solution, indicating its intermolecular character. Analysis of the C=O region (1600–1850 cm^{-1}) confirms this conclusion. A small fragment of Boc-L-Phe-D-Oxd-OBn was examined under a scanning electron microscope (SEM, Figure 23b). Interestingly, the thicknesses and the widths of the mature filaments are almost constant, regardless of the solvent conditions for assembly, whereas their lengths vary widely even under a single set of experimental conditions. The material is stable. Its overall shape was conserved in the precipitation media for several months and even after it had been air-dried. Only strong thermal treatment, such as by an electron beam, provoked the disintegration of the material.

The highly birefringent fibre-like material was analysed by X-ray diffraction (XRD) with use of beams of two different sizes. When a beam size of 200 μm was used, it showed a strong fibre-like XRD pattern that indicates a preferential orientation of crystalline units along the long axis. The use of a narrow X-ray beam (50 μm) or the selection of a small bundle fragment showed diffraction patterns typical of single crystals.

Crystals suitable for a X-ray diffraction study were grown by slow evaporation of a solution of Boc-L-Phe-D-Oxd-OBn in diethyl ether at room temperature. Interestingly, linear chains are formed in the crystal packing of Boc-L-Phe-D-Oxd-OBn through the action of only one intermolecular hydrogen bond between units (Figure 24).

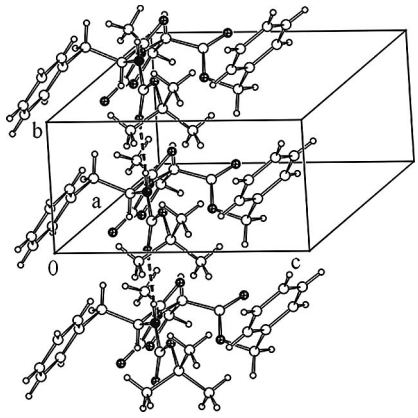

Figure 24. Crystal packing of Boc-L-Phe-D-Oxd-OBn showing one chain running along the *b* axis generated by a single NH···O=C interaction between the molecules. Reproduced from ref.[81]

Finally, fibres of Boc-L-Phe-D-Oxd-OBn were also analysed by solid-state NMR spectroscopy. Narrow NMR lines indicate a highly homogeneous preparation. Qualitative structure information can be obtained from these spectra[82] and confirms that these fibres show a tendency towards a β sheet structure.[83] These results were also confirmed by a systematic conformation analysis at the B3LYP/6–311+G(2d,p) and HF/6–31G* levels of ab initio MO theory.

In conclusion, the solid-state structure of Boc-L-Phe-D-Oxd-OBn can be considered a borderline case of a parallel β sheet structure;[84] indeed, all the examples reported in the literature show fibre-forming peptides that are stabilized in the solid state by at least two N–H···O=C hydrogen bonds. In contrast, this fibre-like material is stabilized only by single hydrogen bonds between dipeptide units.

4.1.2. Boc-L-Phe-D-Imz-OBn

This compound is similar to Boc-L-Phe-D-Oxd-OBn, but contains an additional NH group in the heterocyclic ring, oriented nearly orthogonal to the pre-existing one (Figure 25).[85]

The presence of two NH hydrogen bonds that are not oriented along the same axis should favour the formation of a two-dimensional arrangement. This effect should lead to the formation of layers rather than the fibres obtained with Boc-L-Phe-D-Oxd-OBn, which can form only one hydrogen bond. The synthesis is described in Section 1.4.4. The conformation of Boc-L-Phe-D-Imz-OBn was analysed both in solution and in the solid state. A first analysis was performed by comparing the IR spectrum of a solution (3 mM) in dichloromethane with that of a mixture in KBr (1%). Whereas hydrogen bonding is clearly present in the

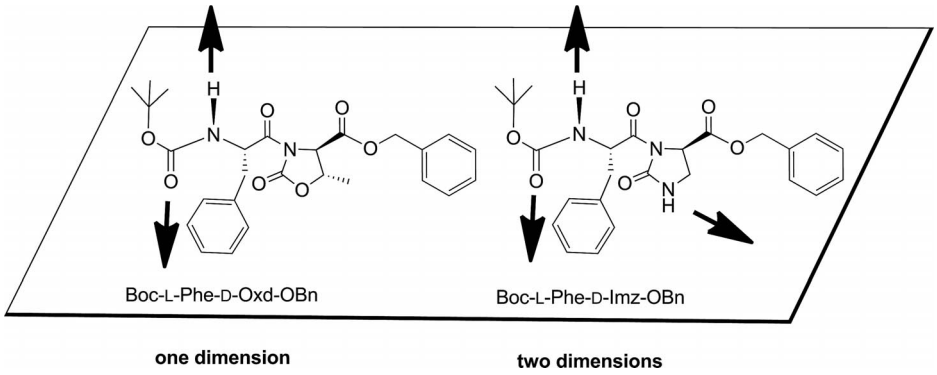

Figure 25. Structural comparison of Boc-L-Phe-D-Oxd-OBn and Boc-L-Phe-D-Imz-OBn.

solid state, as shown by two peaks (3391 and 3371 cm^{-1}) belonging to a broad band, no hydrogen bonding is present in the dilute solution (3444 cm^{-1}), and so intramolecular NH hydrogen bonds are absent. The pronounced variation of the spectrum in the CO region confirms this result.

Several attempts were made to obtain structures that were macroscopically ordered in the solid state by slow evaporation of solutions of Boc-L-Phe-D-Imz-OBn in different solvents.

In contrast with the behaviour of Boc-L-Phe-D-Oxd-OBn, only slow evaporation from protonated solvents such as methanol, ethanol and propan-2-ol provided crystals useful for single-crystal X-ray diffraction studies. Interestingly, the nature of the alcohol has an influence on the preferential elongation and macroscopic side-aggregation of the crystals (Figure 26), but they all show a common tendency to aggregate laterally along their main axes.

The formation of these plate-like crystals only on slow evaporation of protonated solvents suggests that the solvents might play active roles in crystal formation.[86] The obtained single crystals were analysed by X-ray diffraction (XRD). Crystals of Boc-L-Phe-D-Imz-OBn grown from methanol and ethanol show the formation of methanol and ethanol solvates, respectively. In addition to the solvent, two independent molecules of Boc-L-Phe-D-Imz-OBn are present in the unit cell (Figure 27).

As a result of these inter-chain interactions also involving the methanol molecule, the solid-state arrangement of Boc-L-Phe-D-Imz-OBn grown from methanol can be described as a 2D network made of layers, which are parallel to the *ab* plane. The single-crystal X-ray diffraction study carried out on crystals of Boc-L-Phe-D-Imz-OBn grown from ethanol shows the formation of an ethanol solvate isostructural with the methanol solvate, so the two crystal packings are almost identical. In each case the peptide crystallizes in infinite chains with the peptide monomers in a parallel arrangement connected by single hydrogen bonds. The chains are in antiparallel orientation and cross-linked by hydrogen bonds based on the heterocyclic NH group of the D-Imz ring. A 2D network made of layers parallel to the *ab* plane consequently results, producing a "plywood" structure.

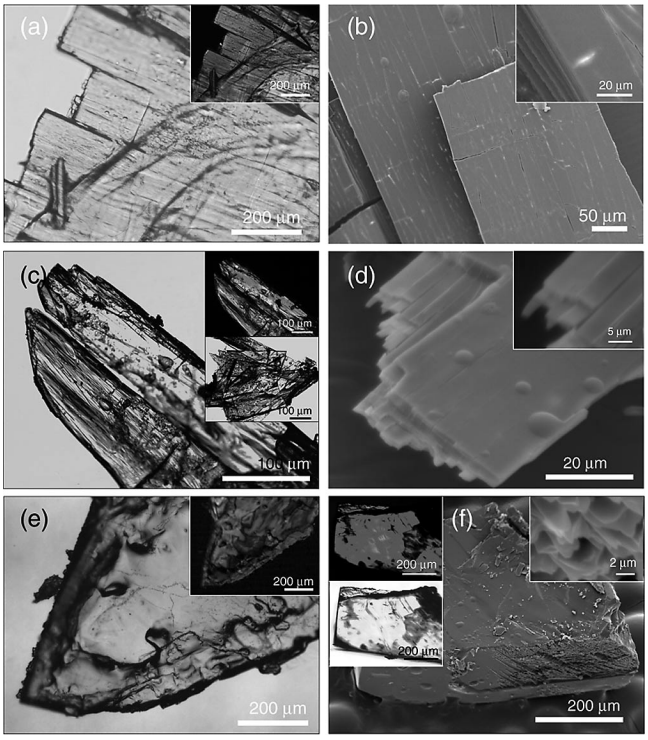

Figure 26. Optical micrographs of crystals of Boc-L-Phe-D-Imz-OBn precipitated by slow evaporation from solutions: (a) from methanol, (c) from ethanol and (e) from propan-2-ol. Scanning electron microscopy images of crystals of Boc-L-Phe-D-Imz-OBn precipitated (b) from methanol, (d) from ethanol and (f) from propan-2-ol. Reprinted with permission from ref.[85] Copyright 2011 American Chemical Society.

A crystal suitable for single-crystal X-ray diffraction studies could also be obtained from propan-2-ol. In this case, no solvent molecules are involved in the crystal structure, probably as a result of the larger size of the propan-2-ol molecule, which can no longer be accommodated in the cavity between two molecules of Boc-L-Phe-D-Imz-OBn. Two different types of intermolecular hydrogen bonds are present in the crystal packing (Figure 28): one hydrogen bond connects the amidic NH hydrogen of the L-Phe unit with the carbonyl oxygen of the CO group of the D-Imz

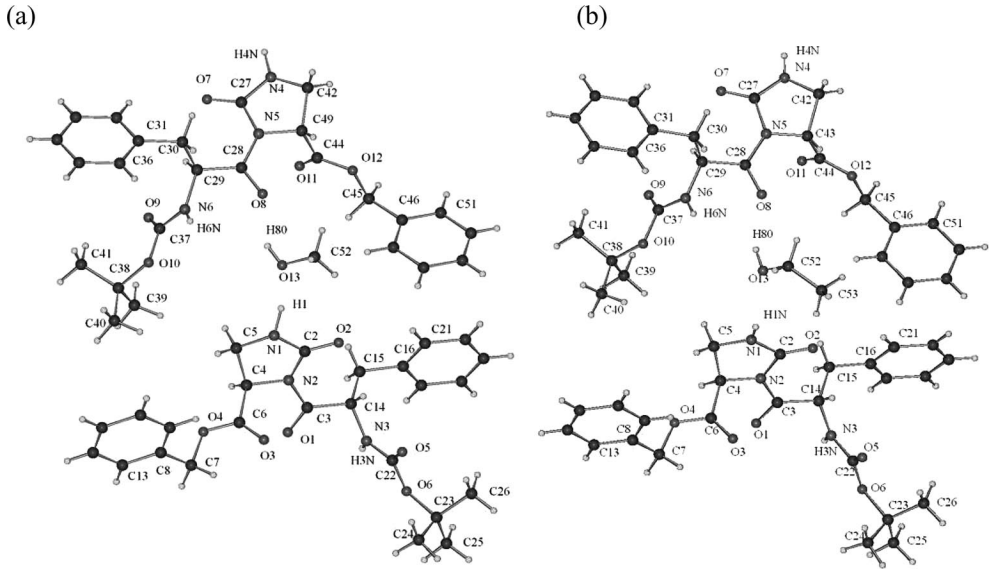

Figure 27. Views of the contents of the unit cells of Boc-L-Phe-D-Imz-OBn crystallized (a) from methanol and (b) from ethanol. Reprinted with permission from ref.[85] Copyright 2011 American Chemical Society.

moiety belonging to another peptide molecule, whereas the other involves the NH proton of the D-Imz ring and the carbonyl oxygen of a *tert*-Boc group of another peptide molecule. These weak interactions also generate a 2D network parallel to the *ab* plane, different from that observed in the packing of Boc-L-Phe-D-Imz-OBn both from methanol and from ethanol. The degree of order in crystal assembly decreases continuously from methanol to ethanol and propan-2-ol.

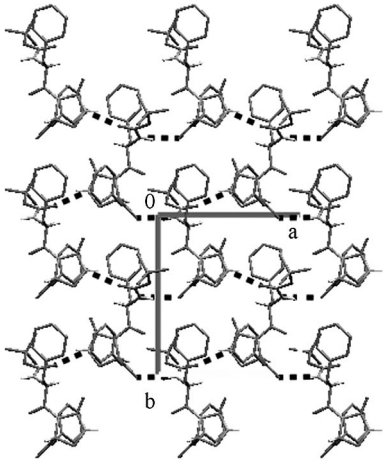

Figure 28. View (down the *c* axis) of the crystal packing of Boc-L-Phe-D-Imz-OBn grown from propan-2-ol. Reprinted with permission from ref.[85] Copyright 2011 American Chemical Society.

4.2. Supramolecular Materials from Tripeptides

This section describes the self-assembly of two epimers Boc-L-Phe-D-Oxd-(*S*)-β^3-hPhg-OBn and Boc-L-Phe-D-Oxd-(*R*)-β^3-hPhg-OBn (Figure 29).[87] These molecules both contain the L-Phe-D-Oxd scaffold, but differ in containing the two enantiomers of β^3-homophenylglycine. The reversal of the stereogenic centre in these moieties has important effects on the preferred molecular conformations and, as a result, on the crystals' morphologies. The two epimers can be prepared by the methods reported in Section 1.

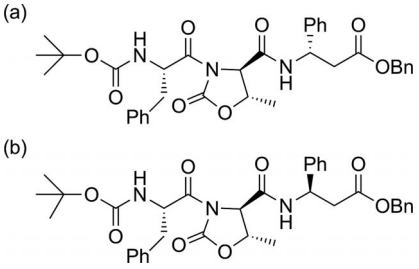

Figure 29. Chemical structures of (a) Boc-L-Phe-D-Oxd-(*S*)-β^3-hPhg-OBn and (b) Boc-L-Phe-D-Oxd-(*R*)-β^3-hPhg-OBn.

The preferred conformations assumed by the two compounds in dilute solutions (3 mM) were analysed by FTIR spectroscopy. Interestingly, Boc-L-Phe-D-Oxd-(*R*)-β^3-hPhg-OBn shows the presence of a NH···O=C hydrogen bond (peaks centred at 3434 and 1670 cm^{-1}), thus suggesting the formation of a γ turn structure, whereas Boc-L-Phe-D-Oxd-(*S*)-β^3-hPhg-OBn does not. This outcome was confirmed by solution NMR spectroscopy, in which the [D$_6$]DMSO dependence of the NH proton chemical shifts was investigated.

In the solid state, in contrast, Boc-L-Phe-D-Oxd-(*S*)-β^3-*h*Phg-OBn and Boc-L-Phe-D-Oxd-(*R*)-β^3-*h*Phg-OBn show very similar IR spectra, with all the NH hydrogen atoms forming NH···O=C hydrogen bonds and all the stretching signals being below 3400 cm^{-1}.

Different modes of aggregation in the solid state would be expected for the epimers, because one tends to form a γ turn structure in solution, whereas the other does not. For

this reason, analysis of the two compounds by microscopy and X-ray diffraction was carried out.

A wide morphological variety of samples based on the compounds Boc-L-Phe-D-Oxd-(*S*)-β^3-*h*Phg-OBn and Boc-L-Phe-D-Oxd-(*R*)-β^3-*h*Phg-OBn and obtained by evaporation from different solvents were analysed by optical and electronic microscopy. These materials always showed birefringence, suggesting high crystallinity (Figure 30). Crystals of Boc-L-Phe-D-Oxd-(*S*)-β^3-*h*Phg-OBn that had been precipitated from methanol appeared elongated in one direction with a hexagonal cross-section. Their lengths varied from one crystal to another over a range of several hundred micrometres, whereas their thicknesses were almost constant around 20 μm. Crystals of Boc-L-Phe-D-Oxd-(*R*)-β^3-*h*Phg-OBn that had been precipitated from ethanol showed an irregular morphology in which plate-like shapes were visible on observation by scanning electron microscopy.

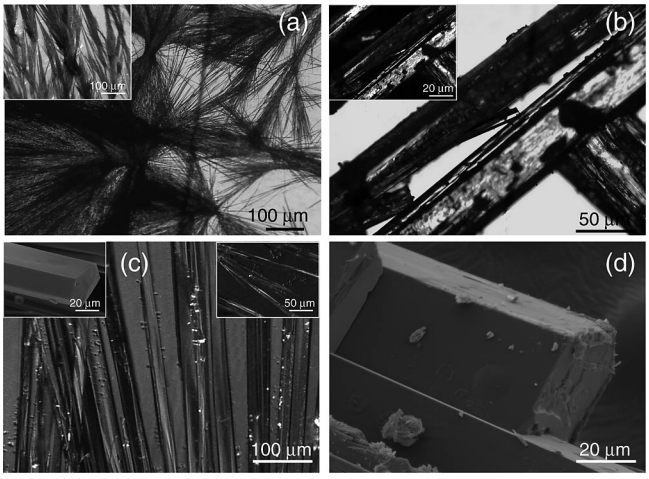

Figure 30. Crystals of Boc-L-Phe-D-Oxd-(*S*)-β^3-*h*Phg-OBn that had been precipitated from ethanol, observed with (a) an optical and (c) an electron microscope. Crystals of Boc-L-Phe-D-Oxd-(*R*)-β^3-*h*Phg-OBn that had been precipitated from ethanol observed with (b) an optical and (d) an electron microscope. Reprinted with permission from ref.[87] Copyright 2011 American Chemical Society.

Crystals suitable for X-ray diffraction study were grown by slow evaporation of solutions of Boc-L-Phe-D-Oxd-(*S*)-β^3-*h*Phg-OBn in methanol and of Boc-L-Phe-D-Oxd-(*R*)-β^3-*h*Phg-OBn in ethanol, both at room temperature. The two molecules are epimers and, as a consequence of this different stereogenic centre, Boc-L-Phe-D-Oxd-(*R*)-β^3-*h*Phg-OBn has a higher degree of folding than Boc-L-Phe-D-Oxd-(*S*)-β^3-*h*Phg-OBn, but no classical intramolecular hydrogen bond is observed in either epimer.

In Boc-L-Phe-D-Oxd-(*S*)-β^3-*h*Phg-OBn crystals, each molecule is engaged in two intermolecular hydrogen bonds with its two neighbours but the two interactions are not equivalent because one is between an amide hydrogen of one side chain and a carbonyl oxygen of the other amide moiety and the second is between the second amide hydrogen and the carbonyl oxygen of the Oxd ring. The crystal packing therefore consists of parallel chains with a helical arrangement (Figure 31) running along the *c* axis. The formation of a ternary helix in the solid state is consistent with the SEM analysis, because the crystals of Boc-L-Phe-D-Oxd-(*S*)-β^3-*h*Phg-OBn from methanol appear elongated in one direction with a hexagonal cross-section.

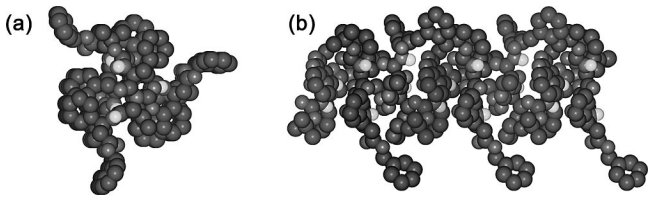

Figure 31. Space-filling model showing the helical arrangement of a chain of Boc-L-Phe-D-Oxd-(*S*)-β^3-*h*Phg-OBn: (a) top view and (b) view along the *c* axis. The molecules are represented in different colours for clarity. The hydrogen atoms involved in H bonding are represented as white cups. Reprinted with permission from ref.[87] Copyright 2011 American Chemical Society.

A completely different packing was observed for the epimer Boc-L-Phe-D-Oxd-(*R*)-β^3-*h*Phg-OBn (Figure 32). This maintains one intermolecular NH···CO hydrogen bond between equivalent amide groups, as observed in Boc-L-Phe-D-Oxd-OBn, but in addition, a second weak hydrogen bond is established between the amide hydrogen of the second amide group and the uncoordinated carboxylic oxygen bearing the Bn group. Although these interactions are weak in comparison with those found in Boc-L-Phe-D-Oxd-OBn, the hydrogen bonding pattern in the crystal lattice shows the formation of infinite parallel β sheets running along the *a* axis.

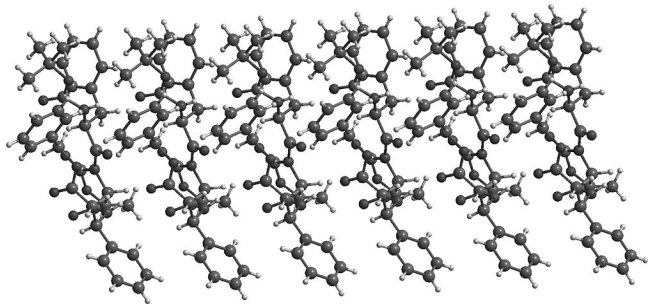

Figure 32. View (down the *c* axis) of the crystal packing of Boc-L-Phe-D-Oxd-(*R*)-β^3-*h*Phg-OBn. Reprinted with permission from ref.[87] Copyright 2011 American Chemical Society.

In conclusion, the reversal of the absolute configuration of the stereogenic centre of the *h*Phg moiety results in a dramatic variation of the preferred conformations of the two compounds, which in turn induces different crystal packings and consequently different crystal morphologies. Boc-L-Phe-D-Oxd-(*S*)-β^3-*h*Phg-OBn forms a ternary helix that crystallizes in hexagonal elongated crystals, whereas

Boc-L-Phe-D-Oxd-(*R*)-β^3-*h*Phg-OBn forms a β sheet structure that crystallizes in different polymorphs, depending on the evaporation solvent.

4.3. Supramolecular Materials from Longer Oligomers

Conformation analysis of Boc-(L-Phe-D-Oxd)$_n$-OBn (n = 2–5) in solution is described in Section 2.2.3. The properties of the solid materials are described here.[67]

The compounds Boc-(L-Phe-D-Oxd)$_n$-OBn (n = 2–5) were analysed by microscopy techniques. All samples were prepared by overnight evaporation of solutions of each compound (50 mg) in a cyclohexane/ethyl acetate mixture (1:1, 1 mL). Only in the case of Boc-(L-Phe-D-Oxd)$_2$-OBn was the formation of a white solid composed of microscopic fibre-like crystals observed by optical microscopy. These crystals clearly showed a preferred direction of growth and formed a highly crystalline material, as shown by their high birefringence. These crystals can reach millimetre lengths and are a few micrometres wide. The optical observation of longer oligomers shows no crystalline habit, and birefringence under crossed polarizers is always absent.

The solid-state oligomers were also analysed by scanning electron microscopy (SEM) and transmission electron microscopy (TEM). The most important results are shown in Figure 33. The filamentous crystals of Boc-(L-Phe-D-Oxd)$_2$-OBn cluster in parallel in closely packed bundles, whereas Boc-(L-Phe-D-Oxd)$_3$-OBn does not form a precipitate of crystalline habit, although filamentous structures are visible on its surface. Indeed, the TEM analysis highlighted the presence of fibrous material dispersed in an amorphous precipitate. These fibres have a ribbon-like structure with a width of 10–15 nm and appear very thin. They are branched and tend to form aggregates.

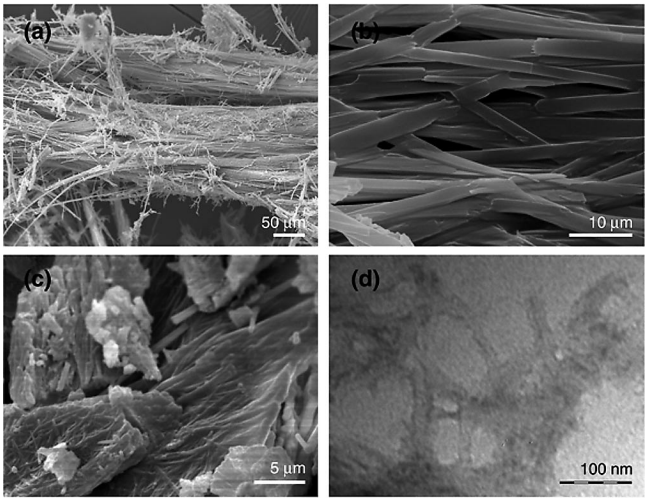

Figure 33. (a) and (b) SEM pictures of Boc-(L-Phe-D-Oxd)$_2$-OBn. (c) SEM and (d) TEM pictures of Boc-(L-Phe-D-Oxd)$_3$-OBn. Reproduced from ref.[67]

The oligomers Boc-(L-Phe-D-Oxd)$_4$-OBn and Boc-(L-Phe-D-Oxd)$_5$-OBn formed materials in which no features typical of crystals or fibres could be observed on inspection either by SEM or by TEM.

Deeper inspection of the behaviour in the solid state was achieved by X-ray powder diffraction analysis. The experimental data clearly indicate that the Boc-(L-Phe-D-Oxd)$_n$-OBn oligomers progressively reduce their degree of order in the solid state with increasing chain length. Obviously, the intermolecular interactions become weaker and are less specific, favouring disordered aggregation of the molecules in the precipitates.

The X-ray molecular structure of Boc-(L-Phe-D-Oxd)$_2$-OBn shows some similarity with the already reported structure of the monomer unit Boc-L-Phe-D-Oxd-OBn. There is only a single intermolecular NH···CO hydrogen bond between the dimeric units in the crystal packing (Figure 34) and it generates an infinite antiparallel β sheet structure running along the crystallographic *a* axis.

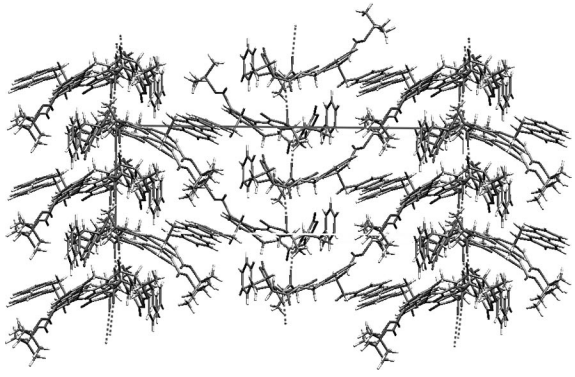

Figure 34. View (down the crystallographic *b* axis) of the crystal packing of Boc-(L-Phe-D-Oxd)$_2$-OBn showing the intermolecular NH···CO hydrogen bonds running along the *a* axis. Reproduced from ref.[67]

Further structural information on the compounds Boc-(L-Phe-D-Oxd)$_2$-OBn (containing 10% U-^{13}C-enriched Phe) was provided by solid-state ^{13}C CPMAS NMR spectroscopy. Distinct chemical shifts and linewidth changes of the amino acid signals can be observed for the individual foldamers. Most prominent are the C_α and C_β signals of the ^{13}C-labelled Phe at about 55 and 40 ppm, respectively. Most intriguing are the changes in linewidth. Whereas Boc-(L-Phe-D-Oxd)$_2$-OBn features narrow lines (of the order of 1 ppm), significantly larger linewidths are observed for the higher oligomers. In contrast, the isotropic chemical shift changes are moderate. Interestingly, Boc-(L-Phe-D-Oxd)$_2$-OBn shows two signals of equal height for the C_α atoms of L-Phe. Increased linewidths of NMR signals are indicative of structural heterogeneity or molecular dynamics. Therefore, the motion-averaged ^{13}C–^{1}H dipolar couplings of the C_α and C_β signals can be measured in the foldamers by use of the DIPSHIFT pulse sequence and the results indicate that the increasing of linewidths of the higher-order foldamers are due to structural heterogeneity.

To provide further information on the preferred secondary structures in the oligomer series, quantum chemical calculations employing ab initio MO theory at various approximation levels were performed. The experimental results provide no convincing indications of ordered structures in Boc-(L-Phe-D-Oxd)$_3$-OBn and Boc-(L-Phe-D-Oxd)$_4$-OBn.

In contrast, both IR and NMR indicate that all the peptidic hydrogen atoms in Boc-(L-Phe-D-Oxd)$_5$-OBn are involved in intramolecular hydrogen bonds, indicating the formation of a secondary structure. As a result of the restriction of the ϕ torsion angle of the D-Oxd constituent to about 60°, two conformational alternatives fulfil the requirements for a regular intramolecular hydrogen bonding pattern (Figure 35).

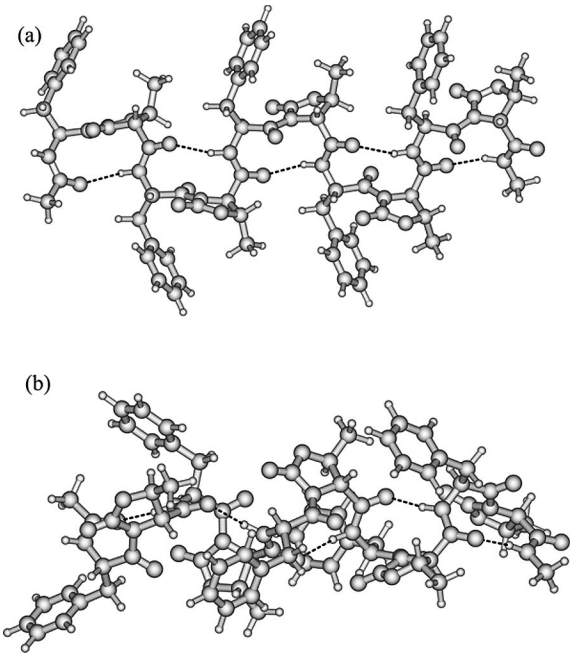

Figure 35. HF/6–31G* structures of Boc-(L-Phe-D-Oxd)$_5$-OBn: (a) poly-β*II*-turn arrangement and (b) poly-βI′-turn arrangement. Reproduced from ref.[67]

The stabilities of both conformers are not very different from those of the two most stable ones observed in the dimer structure. The first conformer (a) corresponds to a βII turn, the second (b) to a distorted βI′(βIII′) turn. The regular poly-βII-turn structure is supported by the NMR spectroscopic data. In contrast, the corresponding values for the most stable poly-βI′ turn structure (b) are distinctly different, with 21.0 ppm at the HF/6–31G* and 21.8 ppm at the B3LYP/6–311+G(2d,p) level. This structure can therefore be excluded not only due to its lower stability, but also by the deviating NMR spectroscopic data.

In conclusion, Boc-(L-Phe-D-Oxd)$_2$-OBn represents a borderline case for an antiparallel β sheet structure, with only one hydrogen bond connecting the peptide molecules. This result is complementary to the crystal structure of Boc-L-Phe-D-Oxd-OBn (Section 4.1.1). In the higher oligomers there is a stronger tendency to form intramolecular rather than intermolecular hydrogen bonds, with the production of amorphous materials. The formation of ordered secondary structures increases and seems to be fully manifested at the pentamer level.

5. Conclusions

This review deals with the synthesis and conformation analysis, as well as some studies as supramolecular materials, of foldamers containing the 4-carboxyoxazolidin-2-one unit or related molecules, in which an imido-type function is obtained by coupling the nitrogen of the heterocycle with the carboxylic acid moiety of the next unit. The imide group is characterized by a nitrogen atom connected to an endocyclic and an exocyclic carbonyl, which tend always to adopt the *trans* conformation. As a consequence of this locally constrained disposition effect, these imide-type oligomers are forced to fold in ordered conformations such as PPII helixes, β band ribbon spirals, β sheets and β or γ turns. Furthermore, a wide variety of unusual secondary structures may be obtained with hybrid foldamers. The behaviour of some of these compounds in the solid state has been analysed in detail, thus showing the formation of different kinds of supramolecular materials that may be used for several applications.

The synthetic approach is highly tuneable with endless variations, so, simply by changing the design and the synthesis, a wide variety of foldamers with the required properties may be prepared "on demand".

Acknowledgments

We thank the Ministero dell'Università e della Ricerca Scientifica (PRIN 2008), the Università di Bologna and the Fondazione del Monte di Bologna e di Ravenna for financial support.

[1] S. H. Gellman, *Acc. Chem. Res.* **1998**, *31*, 173–180.
[2] a) D. J. Hill, M. J. Mio, R. B. Prince, T. S. Hughes, J. S. Moore, *Chem. Rev.* **2001**, *101*, 3893–4011; b) R. P. Cheng, S. H. Gellman, W. F. DeGrado, *Chem. Rev.* **2001**, *101*, 3219–3232; c) M. S. Cubberley, B. L. Iverson, *Curr. Opin. Chem. Biol.* **2001**, *5*, 650–653; d) A. Sanford, B. Gong, *Curr. Org. Chem.* **2003**, *7*, 1649–1659; e) I. Huc, *Eur. J. Org. Chem.* **2004**, *1*, 17–29; f) D. Seebach, A. K. Beck, D. J. Bierbaum, *Chem. Biodiv.* **2004**, *1*, 1111–1239; g) A. R. Sanford, K. Yamato, X. Yang, L. Yuan, Y. Han, B. Gong, *Eur. J. Biochem.* **2004**, *271*, 1416–1425; h) R. P. Cheng, *Curr. Op. Struct. Biol.* **2004**, *14*, 512–520; i) M. A. Balbo Block, C. Kaiser, A. Khan, S. Hecht, *Top. Curr. Chem.* **2005**, *245*, 89–150; j) X. Li, D. Yang, *Chem. Commun.* **2006**, *32*, 3367–3379; k) F. Fulop, T. A. Martinek, G. K. Toth, *Chem. Soc. Rev.* **2006**, *35*, 323–334; l) C. M. Goodman, S. Choi, S. Shandler, W. F. DeGrado, *Nat. Chem. Biol.* **2007**, *3*, 252–262; m) A. D. Bautista, C. J. Craig, E. A. Harker, A. Schepartz, *Curr. Opin. Chem. Biol.* **2007**, *11*, 685–692; n) R. A. Smaldone, J. S. Moore, *Chem. Eur. J.* **2008**, *14*, 2650–2657; o) W. S. Horne, S. H. Gellman, *Acc. Chem. Res.* **2008**, *41*, 1399–1408; p) D. Seebach, J. Gardiner, *Acc. Chem. Res.* **2008**, *41*, 1366–1375; q) I. Saraogi, A. D. Hamilton, *Chem. Soc. Rev.* **2009**, *38*, 1726–1743; r) *Foldamers: Structure, Properties, and Applications* (Eds.: S. Hecht, I. Huc), Wiley-VCH, Weinheim, **2007**.

[3] a) M. Rueping, Y. R. Mahajan, B. Jaun, D. Seebach, *Chem. Eur. J.* **2004**, *10*, 1607–1615; b) D. Seebach, D. F. Hook, A. Glattli, *Biopolymers Peptide Science* **2006**, *84*, 23–37; c) S. J. Wezenberg, G. A. Metselaar, A. E. Rowan, J. J. L. M. Cornelissen, D. Seebach, R. J. M. Nolte, *Chem. Eur. J.* **2006**, *12*, 2778–2786; d) L. Fabian, A. Kalman, G. Argay, G. Bernath, Z. C. Gyarmati, *Cryst. Growth Des.* **2005**, *5*, 773–782; e) T. A. Martinek, A. Hetnyi, L. Fulop, I. M. Mandity, G. K. Toth, I. Dekany, F. Fulop, *Angew. Chem.* **2006**, *118*, 2456; *Angew. Chem. Int. Ed.* **2006**, *45*, 2396–2400; f) A. Hetenyi, Z. Szakonyi, I. Mandity, E. Szolnoki, G. K. Toth, T. A. Martinek, F. Fulop, *Chem. Commun.* **2009**, 177–179; g) T. A. Martinek, I. M. Mandity, L. Fulop, G. K. Toth, E. Vass, Hollosi, E. Forro, F. Fulop, *J. Am. Chem. Soc.* **2006**, *128*, 13539–13544; h) I. M. Mandity, E. Wéber, T. A. Martinek, G. Olajos, G. K. Toth, E. Vass, F. Fulop, *Angew. Chem.* **2009**, *121*, 2205; *Angew. Chem. Int. Ed.* **2009**, *48*, 2171–2175.

[4] P. I. Arvidsson, N. S. Ryder, H. M. Weiss, D. F. Hook, J. Escalante, D. Seebach, *Chem. Biodiv.* **2005**, *2*, 401–419.

[5] a) P. K. Baruah, N. K. Sreedevi, R. Gonnade, S. Ravindranathan, K. Damodaran, H.-J. Hofmann, G. J. Sanjayan, *J. Org. Chem.* **2007**, *72*, 636–639; b) P. Schramm, G. V. M. Sharma, H.-J. Hofmann, *Biopolymers Peptide Science* **2009**, *92*, 279–291; c) G. V. M. Sharma, B. Shoban Babu, K. V. S. Ramakrishna, P. Nagendar, A. C. Kunwar, P. Schramm, C. Baldauf, H.-J. Hofmann, *Chem. Eur. J.* **2009**, *15*, 5552–5566; d) G. V. M. Sharma, N. Chandramouli, M. Choudhary, P. Nagendar, K. V. S. Ramakrishna, A. C. Kunwar, P. Schramm, H.-J. Hofmann, *J. Am. Chem. Soc.* **2009**, *131*, 17335–17344.

[6] a) A. Wittelsberger, M. Keller, L. Scarpellino, L. Patiny, H. Acha-Orbea, M. Mutter, *Angew. Chem.* **2000**, *112*, 1153; *Angew. Chem. Int. Ed.* **2000**, *39*, 1111–1115; b) M. Mutter, T. Haack, *Tetrahedron Lett.* **1992**, *33*, 1589–1592; c) J. P. Tam, Z. Miao, *J. Am. Chem. Soc.* **1999**, *121*, 9013–9022; d) M. Kümin, L.-S. Sonntag, H. Wennemers, *J. Am. Chem. Soc.* **2007**, *129*, 466–467; e) M. Keller, C. Sager, P. Dumy, M. Schutkowski, G. S. Fischer, M. Mutter, *J. Am. Chem. Soc.* **1998**, *120*, 2714–2720; f) P. Dumy, M. Keller, D. E. Ryan, B. Rohwedder, T. Wo, M. Mutter, *J. Am. Chem. Soc.* **1997**, *119*, 918–925; g) M. Mutter, A. Chandravarkar, C. Boyat, J. Lopez, S. Dos Santos, B. Mandal, R. Mimna, K. Murat, L. Patiny, L. Saucède, G. Tuchscherer, *Angew. Chem.* **2004**, *116*, 4267; *Angew. Chem. Int. Ed.* **2004**, *43*, 4172–4178; h) G. Tuchscherer, M. Mutter, *J. Pept. Sci.* **2005**, *11*, 278–282; i) Y. K. Kang, H. S. Park, B. J. Byun, *Biopolymers* **2009**, *91*, 444–455.

[7] G. Chaume, O. Barbeau, P. Lesot, T. Brigaud, *J. Org. Chem.* **2010**, *75*, 4135–4145.

[8] S. K. Panday, J. Prasad, D. K. Dikshit, *Tetrahedron: Asymmetry* **2009**, *20*, 1581–1632.

[9] a) A. L. Johnson, W. A. Price, P. C. Wong, R. F. Vavala, J. M. Stump, *J. Med. Chem.* **1985**, *28*, 1596–1602; b) D. B. Miller, J. H. C. Nayler, H. R. J. Waddington, *J. Chem. Soc. C* **1968**, 242–245; c) G. Osapay, P. Kormoczy, I. Szilagyi, J. Kaitàr, B. Kiss, *Pharmazie* **1990**, *45*, 666–668; d) D. S. Kemp, E. S. Wesley, *Tetrahedron Lett.* **1988**, *29*, 5057–5060; e) B. Rigo, C. Lespagnol, M. Pauly, *J. Heterocycl. Chem.* **1988**, *25*, 49–63; f) B. Rigo, B. Erb, S. E. Ghammarti, P. Gautret, D. J. Couturier, *J. Heterocycl. Chem.* **1995**, *32*, 1599–1604.

[10] a) G. Zappia, G. Cancelliere, E. Gacs-Baitz, G. Delle Monache, D. Misiti, L. Nevola, B. Botta, *Curr. Org. Synth.* **2007**, *4*, 238–307; b) G. Zappia, E. Gacs-Baitz, G. Delle Monache, D. Misiti, L. Nevola, B. Botta, *Curr. Org. Synth.* **2007**, *4*, 81–135; c) G. Zappia, P. Menendez, G. Delle Monache, D. Misiti, L. Nevola, B. Botta, *Mini-Rev. Med. Chem.* **2007**, *7*, 389–409; d) G. Wang, *Anti-Infect. Agents Med. Chem.* **2008**, *7*, 32–49.

[11] a) S. M. Newman, A. Kutner, *J. Am. Chem. Soc.* **1951**, *73*, 4199–4204; b) J. B. Hyne, *J. Am. Chem. Soc.* **1959**, *81*, 6058–6061; c) W. D. Lubell, H. Rapoport, *J. Org. Chem.* **1989**, *54*, 3824–3831; d) D. J. Ager, I. Prakash, D. R. Schaad, *Chem. Rev.* **1996**, *96*, 835–876.

[12] S. Bergmeier, *Tetrahedron* **2000**, *56*, 2561–2576.

[13] E. Falb, A. Nudelman, A. Hassner, *Synth. Commun.* **1993**, *23*, 2839–2844.

[14] a) C. Tomasini, A. Vecchione, *Org. Lett.* **1999**, *1*, 2153–32156.

[15] a) E. Juaristi (Ed.), "*Enantioselective Synthesis of β-Amino Acids*" Wiley-VCH, New York, **1997**; b) D. C. Cole, *Tetrahedron* **1984**, *50*, 9517–9582; c) E. Juaristi, D. Quintana, J. Escalante, *Aldrichimica Acta* **1994**, *27*, 3–11; d) G. Cardillo, C. Tomasini, *Chem. Soc. Rev.* **1996**, *25*, 117–128.

[16] a) H. M. I. Osborn, J. Sweeney, *Tetrahedron: Asymmetry* **1997**, *8*, 1693–1715; b) B. Zwanenburg, L. Thjis, *Pure Appl. Chem.* **1996**, *68*, 735–738; c) D. Tanner, *Angew. Chem.* **1994**, *106*, 625; *Angew. Chem. Int. Ed. Engl.* **1994**, *33*, 599–619; d) P. E. Fanta in *Heterocyclic Compounds with Three- and Four-membered Rings, Part 1* (Ed.: A. Weissberg), Wiley, New York, **1964**, p. 524.

[17] a) D. Seebach, H. Estermann, *Tetrahedron Lett.* **1987**, *28*, 3103–3106; b) D. Seebach, H. Estermann, *Helv. Chim. Acta* **1988**, *71*, 1824–1839; c) G. Cardillo, L. Gentilucci, A. Tolomelli, C. Tomasini, *J. Org. Chem.* **1998**, *63*, 2351–2353; d) G. Cardillo, A. Tolomelli, C. Tomasini, *Eur. J. Org. Chem.* **1999**, 155–161; e) A. M. Nocioni, C. Papa, C. Tomasini, *Tetrahedron Lett.* **1999**, *40*, 8453–8456; f) G. Cardillo, L. Gentilucci, A. Tolomelli, C. Tomasini, *Synlett* **1999**, 1727–1730; g) C. Papa, C. Tomasini, *Eur. J. Org. Chem.* **2000**, 1569–1576.

[18] a) K. Quinze, A. Laurent, P. Mison, *J. Fluorine Chem.* **1989**, *44*, 233–265; b) G. Alvernhe, S. Lacombe, A. Laurent, *Tetrahedron Lett.* **1980**, *21*, 289–292.

[19] D. Ferraris, W. J. Drudy III, C. Cox, T. Lectka, *J. Org. Chem.* **1998**, *63*, 4568–4569.

[20] G. Luppi, C. Tomasini, *Synlett* **2003**, *6*, 797–800.

[21] a) T. Munegumi, Y.-Q. Meng, K. Harada, *Chem. Lett.* **1988**, *10*, 1643–1646; b) J. McGarver, R. N. Hiner, Y. Matsubara, T. Oh, *Tetrahedron Lett.* **1983**, *24*, 2733–2736; c) G. J. McGarvey, J. M. Williams, R. N. Hiner, Y. Matsubara, T. Oh, *J. Am. Chem. Soc.* **1986**, *108*, 4943–4952; d) H. Nitta, I. Ueda, M. Hatanaka, *J. Chem. Soc. Perkin Trans. 1* **1997**, 1793–1798; e) H. Nitta, M. Hatanaka, I. Ueda, *J. Chem. Soc. Perkin Trans. 1* **1990**, 432–433.

[22] Similar behaviour in toluene has recently been described: T. B. Sim, S. H. Kang, K. S. Lee, W. K. Lee, H. Yun, Y. Dong, H.-J. Ha, *J. Org. Chem.* **2003**, *68*, 104–108.

[23] a) P. J. Murray, I. D. Starkey, *Tetrahedron Lett.* **1996**, *37*, 1875–1878; b) D.-C. Ha, K. Kun-Eek, K.-S. Choi, H.-S. Park, *Tetrahedron Lett.* **1996**, *37*, 5723–5726.

[24] a) W. B. Lutz, C. Ressler, D. E. Nettleton Jr., *J. Am. Chem. Soc.* **1959**, *81*, 167–173; b) C. W. Jefford, J. Wang, *Tetrahedron Lett.* **1993**, *34*, 1111–1114; c) J.-I. Park, G. R. Tian, D. H. Kim, *J. Org. Chem.* **2001**, *66*, 3696–3703; d) G. Li, R. Lenington, S. Willis, S. H. Kim, *J. Chem. Soc. Perkin Trans. 1* **1998**, 1753–1754.

[25] G. Luppi, M. Villa, C. Tomasini, *Org. Biomol. Chem.* **2003**, *1*, 247–250.

[26] a) A. W. Hofmann, *Ber. Dtsch. Chem. Ges.* **1881**, *14*, 2725–2736; b) A. W. Hofmann, *Ber. Dtsch. Chem. Ges.* **1885**, *18*, 2734–2741.

[27] a) G. M. Loudon, M. E. Parham, *Tetrahedron Lett.* **1978**, *19*, 437–440; b) M. Waki, Y. Kitajima, N. Zumiya, *Synthesis* **1981**, 266–268; c) P. Pallai, M. Goodman, *J. Chem. Soc., Chem. Commun.* **1982**, 280–281; d) F. Squadrini, A. S. Verdini, G. C. Viscomi, *Gazz. Chim. Ital.* **1984**, *114*, 25–30; e) Y. Shimohigashi, H. Kodama, M. Waki, T. Costa, *Chem. Lett.* **1989**, 1821–1824.

[28] a) E. S. Wallis, J. F. Lane, *Org. React.* **1946**, *3*, 267–306; b) S. Kajigaeshi, K. Asano, S. Fujasaki, T. Kakinami, T. Okamoto, *Chem. Lett.* **1989**, 463–464.

[29] G. Angelici, S. Contaldi, S. L. Green, C. Tomasini, *Org. Biomol. Chem.* **2008**, *6*, 1849–1852.

[30] R. M. Moiarty, *J. Org. Chem.* **2005**, *70*, 2893–2903.

[31] E. Hernandez, J. M. Vèlez, C. P. Vlaar, *Tetrahedron Lett.* **2007**, *48*, 8972–8975.

[32] M. Green, J. Berman, *Tetrahedron Lett.* **1990**, *31*, 5851–5854.
[33] C. Tomasini, M. Villa, *Tetrahedron Lett.* **2001**, *42*, 5211–5214.
[34] S. Lucarini, C. Tomasini, *J. Org. Chem.* **2001**, *66*, 727–800.
[35] N. Xi, M. A. Ciufolini, *Tetrahedron Lett.* **1995**, *36*, 6595–6598.
[36] a) C. G. Fields, D. H. Lloyd, R. L. Macdonald, K. M. Otteson, R. L. Noble, *J. Pept. Res.* **1991**, *4*, 95–101; b) V. Dourtoglou, J.-C. Ziegler, B. Gross, *Tetrahedron Lett.* **1978**, *19*, 1269–1272; c) V. Dourtoglou, B. Gross, V. Lambropoulou, C. Zioudrou, *Synthesis* **1984**, 572–574.
[37] R. M. Kohli, C. T. Walsh, M. D. Burkart, *Nature* **2002**, *418*, 658–661.
[38] a) D. E. Cane, C. T. Walsh, C. Khosla, *Science* **1998**, *282*, 63–68; b) M. A. Marahiel, T. Stachelhaus, H. D. Mootz, *Chem. Rev.* **1997**, *97*, 2651–2674.
[39] For some recent references see: a) J. P. Michael, G. Pattenden, *Angew. Chem.* **1993**, *105*, 1; *Angew. Chem. Int. Ed. Engl.* **1993**, *32*, 1–23; b) A. Bertram, G. Pattenden, *Nat. Prod. Rep.* **2007**, *24*, 18–30; c) A. Bertram, N. Maulucci, O. M. New, S. M. M. Nor, G. Pattenden, *Org. Biomol. Chem.* **2007**, *5*, 1541–1553; d) Y. Hamada, T. Shioiri, *Chem. Rev.* **2005**, *105*, 4441–4482; e) B. S. Davidson, *Chem. Rev.* **1993**, *93*, 1771–1791; f) P. Wipf, *Chem. Rev.* **1995**, *95*, 2115–2134.
[40] G. Angelici, R. Tresanchez Carrera, G. Luppi, C. Tomasini, *Eur. J. Org. Chem.* **2008**, 3552–3558.
[41] a) L. Wang, P. G. Schultz, *Angew. Chem.* **2005**, *117*, 34; *Angew. Chem. Int. Ed.* **2005**, *44*, 34–66; b) D. Summerer, S. Chen, N. Wu, A. Deiters, J. W. Chin, P. G. Schultz, *Proc. Natl. Acad. Sci. USA* **2006**, *103*, 9785–9789; c) S. A. Fleming, J. A. Pincock, *Mol. Supramol. Photochem.* **1999**, 211–281; d) G. Lu, K. Burgess, *Bioorg. Med. Chem. Lett.* **2006**, *16*, 3902–3905.
[42] a) E. Kimura, S. Aoki, E. Kikuta, T. Koike, *Proc. Natl. Acad. Sci. USA* **2003**, *100*, 3731–3736; b) Y. K. Reshetnyak, O. A. Andreev, U. Lehnert, D. M. Engelman, *Proc. Natl. Acad. Sci. USA* **2006**, *103*, 6460–6465; c) P. W. Schiller, I. Berezowska, G. Weltrowska, H. Chen, C. Lemieux, N. N. Chung, *J. Pept. Res.* **2005**, *65*, 556–563; d) G. Balboni, S. Salvadori, A. Dal Piaz, F. Bortolotti, R. Argazzi, L. Negri, R. Lattanzi, S. D. Bryant, Y. Jinsmaa, L. H. Lazarus, *J. Med. Chem.* **2004**, *47*, 6541–6546; e) C. Muller, P. Even, M.-L. Viriot, M.-C. Carre, *Helv. Chim. Acta* **2001**, *84*, 3735–3741.
[43] F. Bernardi, M. Garavelli, M. Scatizzi, C. Tomasini, V. Trigari, M. Crisma, F. Formaggio, C. Peggion, C. Toniolo, *Chem. Eur. J.* **2002**, *8*, 2516–2525.
[44] a) L. J. Bellamy in *The Infrared Spectra of Complex Molecules*, Methuen, London, **1966**; b) W. L. Driessen, P. L. A. Everstijn, *J. Coord. Chem.* **1980**, *10*, 155–158.
[45] D. S. Wishart, B. D. Sykes, F. M. Richards, *J. Mol. Biol.* **1991**, *222*, 311–333.
[46] G. Valle, C. Toniolo, G. Jung, *Liebigs Ann. Chem.* **1986**, 1809–1822.
[47] T. Polonski, *J. Chem. Soc. Perkin Trans. 1* **1988**, 629–637.
[48] A. J. Hopfinger in *Conformational Properties of Macromolecules*, Academic Press, New York, **1973**, pp. 182–189.
[49] a) F. H. Allen, O. Kennard, R. Taylor, *Acc. Chem. Res.* **1983**, *16*, 146–153; b) P. Chakrabarti, S. Chakrabarti, *J. Mol. Biol.* **1998**, *284*, 867–873; c) G. Felcy Fabiola, S. Krishnaswamy, V. Nagarajan, V. Pattabhi, *Acta Crystallogr., Sect. D* **1997**, *53*, 316–320; d) J. Bella, H. M. Berman, *J. Mol. Biol.* **1996**, *264*, 734–742; e) Z. S. Derewenda, L. Lee, V. Derewenda, *J. Mol. Biol.* **1995**, *252*, 248–262; f) T. Steiner, *J. Chem. Soc. Perkin Trans. 2* **1995**, 1315–1319; g) G. R. Desiraju, *Acc. Chem. Res.* **1996**, *29*, 441–449; h) T. Steiner, W. Saenger, *J. Am. Chem. Soc.* **1992**, *114*, 10146–10154; i) G. R. Desiraju, T. Steiner, *The Weak Hydrogen Bond in Structural Chemistry and Biology*, Oxford Science, Oxford, UK, **1999**.
[50] E. Benedetti, A. Bavoso, B. Di Blasio, V. Pavone, C. Pedone, C. Toniolo, G. M. Bonora, *Biopolymers* **1983**, *22*, 305–317.
[51] C. Tomasini, V. Trigari, S. Lucarini, F. Bernardi, M. Garavelli, C. Peggion, F. Formaggio, C. Toniolo, *Eur. J. Org. Chem.* **2003**, 259–267.
[52] Y. Xu, P. Saweczko, H.-B. Kraatz, *J. Organomet. Chem.* **2001**, *637–639*, 335–342.
[53] a) K. Wolinski, J. F. Hilton, P. Pulay, *J. Am. Chem. Soc.* **1990**, *112*, 8251–8260; b) K. Wolinski, A. J. Sadlej, *Mol. Phys.* **1980**, *41*, 1419–1430; c) R. Ditchfield, *Mol. Phys.* **1974**, *27*, 789–807; d) R. McWeeny, *Phys. Rev.* **1962**, *126*, 1028–1024; e) F. London, *J. Phys. Radium* **1937**, *8*, 397–409; f) A. Bagno, *Chem. Eur. J.* **2001**, *7*, 1652–1660.
[54] G. Luppi, R. Galeazzi, M. Garavelli, F. Formaggio, C. Tomasini, *Org. Biomol. Chem.* **2004**, *2*, 2181–2187.
[55] G. Chang, W. C. Guida, W. C. Still, *J. Am. Chem. Soc.* **1989**, *111*, 4379–4386.
[56] a) W. L. Jorgensen, J. Tirado-Rives, *J. Am. Chem. Soc.* **1988**, *110*, 1657–1666; b) J. Pranata, S. G. Wierschke, W. L. Jorgensen, *J. Am. Chem. Soc.* **1991**, *113*, 2810–2819.
[57] W. C. Still, A. Tempczyk, R. C. Hawley, T. Hendrickson, *J. Am. Chem. Soc.* **1990**, *112*, 6127–6129.
[58] G. Luppi, C. Soffrè, C. Tomasini, *Tetrahedron: Asymmetry* **2004**, *15*, 1645–1650.
[59] a) K. D. Kopple, M. Ohnishi, A. Go, *Biochemistry* **1969**, *8*, 4087–4095; b) D. Martin, G. Hauthal in *Dimethyl Sulphoxide*, Van Nostrand–Reinhold, Wokingham, UK, **1975**.
[60] C. Tomasini, G. Luppi, M. Monari, *J. Am. Chem. Soc.* **2006**, *128*, 2410–2420.
[61] a) G. R. Marshall in *Intra-Science Chemistry Report* (Ed.: N. Kharasch), Gordon & Breach, New York, **1971**, pp. 305–316; b) I. L. Karle, P. Balaram, *Biochemistry* **1990**, *29*, 6747–6756; c) C. Toniolo, M. Crisma, F. Formaggio, C. Peggion, *Biopolymers Pept. Sci.* **2001**, *60*, 396–419.
[62] K. Wüthrich in *NMR of Proteins and Nucleic Acids*, Wiley, New York, **1986**, p. 192.
[63] a) A. Glättli, X. Daura, D. Seebach, W. F. van Gunsteren, *J. Am. Chem. Soc.* **2002**, *124*, 12972–12978; b) B. R. Huck, J. D. Fisk, I. A. Guzei, H. A. Carlson, S. H. Gellman, *J. Am. Chem. Soc.* **2003**, *125*, 9035–9037; c) J.-S. Park, H.-S. Lee, J. R. Lai, B. M. Kim, S. H. Gellman, *J. Am. Chem. Soc.* **2003**, *125*, 8539–8545; d) T. L. Raguse, J. R. Lai, S. H. Gellman, *J. Am. Chem. Soc.* **2003**, *125*, 5592–5593; e) S. A. Hart, A. B. F. Bahadoor, E. E. Matthews, X. J. Qiu, A. Schepartz, *J. Am. Chem. Soc.* **2003**, *125*, 4022–4023.
[64] a) C. Toniolo, A. Polese, F. Formaggio, M. Crisma, J. Kamphuis, *J. Am. Chem. Soc.* **1996**, *118*, 2744–2745; b) C. Toniolo, F. Formaggio, S. Tognon, Q. B. Broxterman, B. Kaptein, R. Huang, V. Setnicka, T. A. Keiderling, I. H. McColl, L. Hecht, L. D. Barron, *Biopolymers* **2004**, *75*, 32–45; c) F. Formaggio, C. Baldini, V. Moretto, M. Crisma, B. Kaptein, Q. B. Broxterman, C. Toniolo, *Chem. Eur. J.* **2005**, *11*, 2395–2404.
[65] M. C. Manning, R. W. Woody, *Biopolymers* **1991**, *31*, 569–586.
[66] a) B. V. Venkataram Prasad, P. Balaram, *Int. J. Biol. Macromol.* **1982**, *4*, 99–102; b) B. Di Blasio, V. Pavone, M. Saviano, A. Lombardi, F. Nastri, C. Pedone, E. Benedetti, M. Crisma, M. Anzolin, C. Toniolo, *J. Am. Chem. Soc.* **1992**, *114*, 6273–6278; c) I. Segalas, Y. Prigent, D. Davoust, B. Bodo, S. Rebuffat, *Biopolymers* **1999**, *50*, 71–85; d) I. L. Karle, J. Flippen-Anderson, M. Sukumar, P. Balaram, *Proc. Natl. Acad. Sci. USA* **1987**, *84*, 5087–5091.
[67] G. Angelici, G. Falini, H.-J. Hofmann, D. Huster, M. Monari, C. Tomasini, *Chem. Eur. J.* **2009**, *15*, 8037–8048.
[68] E. Alonso, F. Lopez-Ortiz, C. del Pozo, E. Peralta, A. Macìas, J. Gonzalez, *J. Org. Chem.* **2001**, *66*, 6333–6338.
[69] P. Salvadori, L. Lardicci, R. Menicagli, C. Bertucci, *J. Am. Chem. Soc.* **1972**, *94*, 8598–8600.
[70] G. Angelici, G. Luppi, B. Kaptein, Q. B. Broxterman, H.-J. Hofmann, C. Tomasini, *Eur. J. Org. Chem.* **2007**, 2713–2721.
[71] S. Laschat, H. Kunz, *J. Org. Chem.* **1991**, *56*, 5883–5889.
[72] a) R. W. Woody in *Circular Dichroism, Principles and Applications* (Eds.: K. Nakanishi, N. Berova, R. W. Woody), VCH, New York, **1994**; b) J. W. Nelson, N. R. Kallenbach, *Proteins Struct., Funct., Genet.* **1986**, *1*, 211–217.

[73] a) P. N. Lewis, F. A. Momany, H. A. Scheraga, *Biochem. Biophys. Acta* **1973**, *303*, 211–229; b) P. Y. Chou, G. D. Fasman, *J. Mol. Biol.* **1977**, *115*, 135–175; c) C. M. Wilmot, J. M. Thornton, *J. Mol. Biol.* **1988**, *203*, 211–232.
[74] G. Luppi, D. Lanci, V. Trigari, M. Garavelli, A. Garelli, C. Tomasini, *J. Org. Chem.* **2003**, *68*, 1982–1993.
[75] G. Luppi, A. Garelli, L. Prodi, Q. B. Broxterman, B. Kaptein, C. Tomasini, *Org. Biomol. Chem.* **2005**, *3*, 1520–1524.
[76] F. A. Cotton, G. Wilkinson, *Advanced Inorganic Chemistry*, Wiley, New York, **1988**.
[77] K. I. Varughese, S. Aimoto, G. Kartha, *Int. J. Pept. Prot. Res.* **1986**, *27*, 118–122.
[78] a) F. E. Cohen, J. W. Kelly, *Nature* **2003**, *426*, 905–909; b) J. Sato, T. Takahashi, H. Oshima, S. Matsumura, H. Mihara, *Chem. Eur. J.* **2007**, *13*, 7745–7752; c) R. Mishra, B. Bulic, D. Sellin, S. Jha, H. Waldmann, R. Winter, *Angew. Chem.* **2008**, *120*, 4757–4760; *Angew. Chem. Int. Ed.* **2008**, *47*, 4679–4682.
[79] a) S. Guha, M. G. B. Drew, A. Banerjee, *Chem. Mater.* **2008**, *20*, 2282–2290; b) S. K. Maji, D. Haldar, A. Banerjee, A. Banerjee, *Tetrahedron* **2002**, *58*, 8695–8702; c) S. K. Maji, M. G. B. Drew, A. Banerjee, *Chem. Commun.* **2001**, 1946–1947; d) R. V. Ulijn, A. M. Smith, *Chem. Soc. Rev.* **2008**, *37*, 664–675; e) F. Rúa, S. Boussert, T. Parella, I. Díez-Pérez, V. Branchadell, E. Giralt, R. M. Ortuño, *Org. Lett.* **2007**, *9*, 3643–3645.
[80] I. Cherny, E. Gazit, *Angew. Chem.* **2008**, *120*, 4128–4136; *Angew. Chem. Int. Ed.* **2008**, *47*, 4062–4069.
[81] G. Angelici, G. Falini, H.-J. Hofmann, D. Huster, M. Monari, C. Tomasini, *Angew. Chem.* **2008**, *120*, 8195; *Angew. Chem. Int. Ed.* **2008**, *47*, 8075–8078.
[82] Y. Wang, O. Jardetzky, *Protein Sci.* **2002**, *11*, 852–861.
[83] M. Sackewitz, H. A. Scheidt, G. Lodderstedt, A. Schierhorn, E. Schwarz, D. Huster, *J. Am. Chem. Soc.* **2008**, *130*, 7172–7273.
[84] a) S. Grimme, *Angew. Chem.* **2008**, *120*, 3478–3483; *Angew. Chem. Int. Ed.* **2008**, *47*, 3430–3434; b) E. C. Lee, D. Kim, P. Jurečka, P. Tarakeshwar, P. Hobza, K. S. Kim, *J. Phys. Chem. A* **2007**, *111*, 3446–3457.
[85] G. Angelici, N. Castellucci, S. Contaldi, G. Falini, H.-J. Hofmann, M. Monari, C. Tomasini, *Cryst. Growth Des.* **2010**, *10*, 244–251.
[86] S. Guha, M. G. B. Drew, A. Banerjee, *CrystEngComm* **2009**, *11*, 756–762.
[87] G. Angelici, N. Castellucci, G. Falini, D. Huster, M. Monari, C. Tomasini, *Cryst. Growth Des.* **2010**, *10*, 923–929.

Received: April 7, 2011
Published Online: June 22, 2011

